CHAPTER 5

SOME INVESTIGATIONS ON A RECENT HEAT CONDUCTION MODEL WITH A DELAY

5.1 Analysis of a Recent Heat Conduction Model with a delay for Thermoelastic Interactions in an Unbounded Medium with a Spherical Cavity

5.1.1 Introduction

In this section of the present thesis, we study the thermoelastic interactions in an unbounded medium with a spherical cavity in the context of the, very recently proposed heat conduction model including one single delay term established by Quintanilla (2011). This heat conduction model is a reformulation of three phase-lag heat conduction model and is an alternative heat conduction theory with a single delay term. In the previous chapter, we have established the theorem of the uniqueness of solution, variational principle and a reciprocity relation for this new theory. In the present section, we aim to investigate this model and study the thermoelastic interactions in an isotropic homogeneous elastic medium with a spherical cavity subjected to three types of thermal and mechanical loads in the context of two versions of this new model. Analytical solutions for the distribution of the field variables like, displacement, temperature and stresses are found out with the help of the integral transform technique. A detailed analysis of analytical results is provided by short-time approximation concept. Further, the numerical solutions of the problems are performed by applying numerical inversion of Laplace transform and the illustration is made to analyze the effects of applying this model as compared to other existing heat conduction models. We observe

The content of this section is communicated to an international peer reviewed journal.

significant variation in the analytical results predicted by different heat conduction models. Numerical values of the field variables are also observed to show significantly different results for a particular material. We concluded that the variation in the predictions by different models are greatly dependent on the type of thermomechanical loads. Several important points in this regard are highlighted in the present work.

5.1.2 Governing equations

By following Quintanilla (2011) and Leseduarte and Qunitanilla (2013), we consider the basic governing equations in the absence of body forces and heat sources for an isotropic elastic medium in indicial notation as follows:

Stress-strain-temperature relation:

$$\sigma_{ij} = \lambda e \delta_{ij} + 2\mu e_{ij} - \beta\theta\delta_{ij} \tag{5.1.1}$$

Displacement equation of motion:

$$(\lambda + \mu)\frac{\partial e}{\partial r} - \beta\theta_{,i} = \rho\frac{\partial^2 u_i}{\partial t^2} \tag{5.1.2}$$

Heat conduction equation:

$$\{k\frac{\partial}{\partial t} + k^*(1 + \tau\frac{\partial}{\partial t} + \frac{1}{2}\tau^2\xi\frac{\partial^2}{\partial t^2})\}\theta_{,ii} = \beta\theta_0\frac{\partial^2 e}{\partial t^2} + \rho c_E\frac{\partial^2\theta}{\partial t^2} \tag{5.1.3}$$

Here, τ is the delay term in the reference of the new model given by Quintanilla (2011). The parameter ξ has been used here to formulate the problem under two different models of heat conduction in a unified way. Since the present model given by Quintanilla (2011) is an extension of Green-Naghdi thermoelasticity model hence the case when we assume $\tau = 0$ in equation (5.1.3) corresponds to the heat conduction equation of thermoelasticity under GN-III model. In the case when $\tau \neq 0$, we obtain two different versions of heat conduction equation by Leseduarte and Quintanilla (2013) by assuming

$\xi = 1$ and $\xi = 0$, whereas in the second case (*i.e.*, when $\xi = 0$), we neglect the second order effects in the Taylor series approximation of the equation of heat conduction to the delay term.

Hence, we study our problem by considering equations (5.1.1), (5.1.2) and (5.1.3) to analyze the results under two different cases as follows:

1. **New model – I** : $\tau \neq 0, \xi = 1$
2. **New model – II** : $\tau \neq 0, \xi = 0$

5.1.3 Problem Formulation

We consider an infinitely extended homogeneous isotropic elastic medium with a spherical cavity of radius a. The center of the cavity is taken to be the origin of the spherical polar coordinate system(r,θ, ϕ). By assuming spherical symmetry in our problem, the displacement and temperature components are taken to be functions of r and t only. The non-zero strain components are therefore given by

$$e_{rr} = \frac{\partial u}{\partial r},\ e_{\theta\theta} = e_{\phi\phi} = \frac{u}{r}$$

Then, the non-zero stress components are obtained as

$$\sigma_{rr} = \lambda(\frac{\partial u}{\partial r} + \frac{2u}{r}) + 2\mu\frac{\partial u}{\partial r} - \beta\theta \tag{5.1.4}$$

$$\sigma_{\theta\theta} = \sigma_{\phi\phi} = \lambda(\frac{\partial u}{\partial r} + \frac{2u}{r}) + 2\mu\frac{\mu}{r} - \beta\theta \tag{5.1.5}$$

Hence, the equation of motion (5.1.1) reduces to the form

$$\rho\frac{\partial^2 u}{\partial t^2} = \frac{\partial}{\partial r}\sigma_{rr} + \frac{2}{r}(\sigma_{rr} - \sigma_{\theta\theta}) \tag{5.1.6}$$

Now, for simplicity we introduce the following dimensionless variables and quantities:

$r' = \frac{r}{a},\ t' = \frac{c_1}{a}t,\ \theta' = \frac{\theta}{\theta_0},\ u' = \frac{u}{a},\ \tau' = \frac{c_1}{a}\tau,\ a_0 = \frac{ak^*}{kc_1},\ a_1 = \frac{\beta\theta_0}{\lambda+\mu},$

$a_2 = \frac{a\rho c_E c_1}{k},\ a_3 = \frac{a\beta c_1}{k},\ \sigma'_{rr} = \frac{\sigma_{rr}}{\lambda+2\mu},\ \sigma'_{\phi\phi} = \frac{\sigma_{\phi\phi}}{\lambda+2\mu}$, and $\lambda_1 = \frac{\lambda}{\lambda+2\mu}$.

Then, (5.1.4), (5.1.5) and (5.1.6) reduce to

$$\sigma_{rr} = \frac{\partial u}{\partial r} + 2\lambda_1 \frac{u}{r} - a_1\theta \tag{5.1.7}$$

$$\sigma_{\phi\phi} = \lambda_1 \frac{\partial u}{\partial r} + (\lambda_1 + 1)\frac{u}{r} \tag{5.1.8}$$

$$\frac{\partial^2 u}{\partial t^2} = \frac{\partial e}{\partial r} - a_1 \frac{\partial \theta}{\partial r} \tag{5.1.9}$$

In above equations, we omit the primes for simplicity.

Further, the equation of heat conduction is simplified to the dimensionless form as

$$\{\frac{\partial}{\partial t} + a_0(1 + \tau\frac{\partial}{\partial t} + \frac{1}{2}\tau^2\xi\frac{\partial^2}{\partial t^2})\}\nabla^2\theta = a_3\frac{\partial^2 e}{\partial t^2} + a_2\frac{\partial^2\theta}{\partial t^2} \tag{5.1.10}$$

We consider that the medium is at rest and undisturbed at the beginning and the initial conditions are taken to be homogeneous, i.e., we assume that

$$u(r,t)\mid_{t=0} = \frac{\partial}{\partial t}u(r,t)\mid_{t=0} = 0$$

$$\theta(r,t)\mid_{t=0} = \frac{\partial}{\partial t}\theta(r,t)\mid_{t=0} = 0$$

$$\sigma_{rr}(r,t)\mid_{t=0} = 0$$

5.1.4 Solution of the Problem

We introduce the Laplace transform defined by

$$\bar{f}(r,p) = \int_0^\infty \mathrm{e}^{-pt} f(r,t)dt$$

where p is the Laplace transform parameter.

Therefore, by applying the Laplace transform to equations (5.1.7)-(5.1.10) with respect to time t, we get following equations:

$$\bar{\sigma}_{rr} = \bar{e} - 2(1-\lambda_1)\frac{\bar{u}}{r} - a_1\bar{\theta} \tag{5.1.11}$$

$$\bar{\sigma}_{\phi\phi} = \lambda_1\bar{e} + (1-\lambda_1)\frac{\bar{u}}{r} - a_1\bar{\theta} \tag{5.1.12}$$

$$p^2\bar{u} = \frac{\partial\bar{e}}{\partial r} - a_1\frac{\partial\bar{\theta}}{\partial r} \tag{5.1.13}$$

$$\{p + a_0(1+\tau p + \frac{1}{2}\xi\tau^2p^2)\}\nabla^2\bar{\theta} = a_3p^2\bar{e} + a_2p^2\bar{\theta} \tag{5.1.14}$$

Decoupling equations (5.1.13) and (5.1.14) and solving them, we get the general solutions for $\bar{e}$ and $\bar{\theta}$ bounded at infinity as

$$\bar{e} = \frac{1}{\sqrt{r}}[X_1K_{\frac{1}{2}}(m_1r) + X_2K_{\frac{1}{2}}(m_2r)] \tag{5.1.15}$$

$$\bar{\theta} = \frac{1}{\sqrt{r}}[Y_1K_{\frac{1}{2}}(m_1r) + Y_2K_{\frac{1}{2}}(m_2r)] \tag{5.1.16}$$

Here, X_i, Y_i $(i = 1, 2)$ are the arbitrary constants independent of r, $K_{\frac{1}{2}}(m_ir)$ are modified Bessel functions of order half and m_1, m_2 satisfy the following equation:

$$\begin{aligned}\{p + a_0(1+\tau p + \frac{1}{2}\xi\tau^2p^2)\}m^4 - \\ \{p^3 + \epsilon p^2 + a_2p^2 + a_0p^2(1+\tau p + \frac{1}{2}\xi\tau^2p^2)\}m^2 + a_2p^4 = 0\end{aligned} \tag{5.1.17}$$

Here, $\epsilon = \frac{\beta^2\theta_0}{\rho^2 c_v c_1^2}$ is the thermoelastic coupling constant.

Now, by using (5.1.13), (5.1.15) and (5.1.16), we find the relation between X_i and Y_i as

$$\begin{aligned} Y_i &= F_i X_{i,} \quad \text{for}\, i = 1, 2 \\ \text{where}, F_i &= \frac{m_i^2 - p^2}{a_1 m_i^2}, \ i = 1, 2 \end{aligned} \tag{5.1.18}$$

We apply the relation

$$\frac{d}{dr}K_{\frac{1}{2}}(m_i r) = \frac{1}{2r}K_{\frac{1}{2}}(m_i r) - m_i K_{\frac{3}{2}}(m_i r), \quad \text{for}\, i = 1, 2$$

in order to find the solutions for displacement and stresses from equations (5.1.7)-(5.1.10), (5.1.15) and (5.1.16) as

$$\bar{u} = -\frac{1}{\sqrt{r}}[\frac{1}{m_1}X_1 K_{\frac{3}{2}}(m_1 r) + \frac{1}{m_2}X_2 K_{\frac{3}{2}}(m_2 r)] \tag{5.1.19}$$

$$\bar{\sigma}_{rr} = \frac{1}{\sqrt{r}}[X_1\sigma_{r1} + X_2\sigma_{r2}] \tag{5.1.20}$$

$$\bar{\sigma}_{\phi\phi} = \frac{1}{\sqrt{r}}[X_1\sigma_{\phi 1} + X_2\sigma_{\phi 2}] \tag{5.1.21}$$

where

$$\sigma_{ri} = [1 - a_1 F_i]K_{\frac{1}{2}}(m_i r) + \frac{2(1-\lambda_1)}{m_i r}K_{\frac{3}{2}}(m_i r), \quad i = 1, 2$$

$$\sigma_{\phi i} = [\lambda_1 - a_1 F_i]K_{\frac{1}{2}}(m_i r) - \frac{(1-\lambda_1)}{m_i r}K_{\frac{3}{2}}(m_i r), \quad i = 1, 2$$

We can obtain the values of X_1 and X_2 with the help of the boundary conditions.

5.1.5 Applications

Now, we apply above formulation to investigate the nature of solutions in different cases of thermoelastic interactions. Hence, we consider three problems that correspond to three types of thermal and mechanical boundary conditions as follows:

Problem-1: Ramp-type varying temperature and zero stress on the boundary of the spherical cavity

We consider a homogeneous isotropic thermoelastic solid with homogeneous initial conditions. The surface of the cavity, $r = 1$ is considered to be stress free and is affected by ramp-type heating which depends on time t. Hence, we assume boundary conditions as

$$\sigma_{rr} \mid_{r=1} = 0 \tag{5.1.22}$$

$$\theta \mid_{r=1} = \begin{cases} 0, \ t \leq 0, \\ T_0 \frac{t}{t_0}, \ 0 < t \leq t_0, \\ T_0, \ t > t_0. \end{cases} \tag{5.1.23}$$

where, t_0 indicates the length of time to raise the heat and T_0 is a constant. This means that the boundary of the surface of the cavity, which is initially at rest is suddenly raised to an increased temperature equal to the function $F(t) = T_0 \frac{t}{t_0}$ and after the instance $t = t_0$ coming, we let the temperature at constant value T_0 maintain from then on.

The Laplace transform of equations (5.1.22) and (5.1.23) yields

$$\bar{\sigma}_{rr} \mid_{r=1} = 0 \tag{5.1.24}$$

$$\bar{\theta} \mid_{r=1} = \frac{T_0(1 - e^{-pt_0})}{t_0 p^2} \tag{5.1.25}$$

Therefore, with the help of boundary conditions (5.1.24) and (5.1.25), we find the constants X_1 and X_2 involved in solutions of different field variables in Laplace transform domain as

$X_1 = -\frac{\sigma^0_{r2}T_0(1-e^{-pt_0})}{t_0p^2[\sigma^0_{r1}F_2K_{\frac{1}{2}}(m_2)-\sigma^0_{r2}F_1K_{\frac{1}{2}}(m_1)]}$,

$X_2 = \frac{\sigma^0_{r1}T_0(1-e^{-pt_0})}{t_0p^2[\sigma^0_{r1}F_2K_{\frac{1}{2}}(m_2)-\sigma^0_{r2}F_1K_{\frac{1}{2}}(m_1)]}$

where, $\sigma^0_{ri} = [1 - a_1F_i]K_{\frac{1}{2}}(m_i) + \frac{2(1-\lambda_1)}{m_i}K_{\frac{3}{2}}(m_i), \quad i = 1,2.$

Problem-2: Unit step increase in temperature and zero stress of the boundary of the cavity of the medium

Here, we assume that the surface of the cavity, $r = 1$ is stress free and is subjected to a unit step increase in temperature, i.e. we consider

$$\sigma_{rr} \mid_{r=1} = 0 \tag{5.1.26}$$

$$\theta \mid_{r=1} = T^*H(t), \tag{5.1.27}$$

where, T^* is a constant temperature and $H(t)$ is the Heaviside unit step function.

The Laplace transform of equations (5.1.26), and (5.1.27) are given by

$$\bar{\sigma}_{rr} \mid_{r=1} = 0 \tag{5.1.28}$$

$$\bar{\theta} \mid_{r=1} = \frac{T^*}{p}, \tag{5.1.29}$$

Similarly, with the help of (5.1.28) and (5.1.29), the constants X_1, X_2 are obtained as:

$X_1 = -\frac{\sigma^0_{r2}T^*}{p[\sigma^0_{r1}F_2K_{\frac{1}{2}}(m_2)-\sigma^0_{r2}F_1K_{\frac{1}{2}}(m_1)]}$,

$X_2 = \frac{\sigma^0_{r1}T^*}{p[\sigma^0_{r1}F_2K_{\frac{1}{2}}(m_2)-\sigma^0_{r2}F_1K_{\frac{1}{2}}(m_1)]}$

Problem-3: Normal load on the boundary of the spherical cavity

In this case, we assume that the surface of the cavity is kept at the constant reference temperature, and it is subjected to a normal load. Therefore, the boundary conditions for this problem are of the form

$$\sigma_{rr} \mid_{r=1} = -\sigma^* H(t) \tag{5.1.1.30}$$

$$\theta \mid_{r=1} = 0, \tag{5.1.1.31}$$

Laplace transform of (5.1.30) and (5.1.31) yields

$$\bar{\sigma}_{rr} \mid_{r=1} = -\frac{\sigma^*}{p} \tag{5.1.32}$$

$$\bar{\theta} \mid_{r=1} = 0, \tag{5.1.33}$$

In this case, the constants X_1, X_2 are found to be of the form

$X_1 = \frac{F_2 K_{\frac{1}{2}}(m_2)\sigma^*}{p[\sigma^0_{r2} F_1 K_{\frac{1}{2}}(m_1) - \sigma^0_{r1} F_2 K_{\frac{1}{2}}(m_2)]}$,

$X_2 = -\frac{F_1 K_{\frac{1}{2}}(m_1)\sigma^*}{p[\sigma^0_{r2} F_1 K_{\frac{1}{2}}(m_1) - \sigma^0_{r1} F_2 K_{\frac{1}{2}}(m_2)]}$

5.1.6 Short-Time Approximation

We will find the solutions to the distributions of displacement, temperature and stresses in the physical domain (r, t) by inverting the expressions for $\bar{u}$, $\bar{\theta}$, $\bar{\sigma}_{rr}$, $\bar{\sigma}_{\phi\phi}$ obtained in previous section by using the Laplace inverse transforms. However, these expressions involve complicated functions of Laplace transform parameter, p. Hence, the closed form inversion of Laplace transforms for any value of p is formidable task. Therefore, in this section, we attempt to get the short-time approximated solutions of the field variables in the time domain for small values of time, i.e., for large values of p.

Firstly, with the help of Maclaurin's series expansion and neglecting the higher powers of small terms, we get the roots m_1, m_2 of equation (5.1.17) under different models as follows:

For New Model -I:

$$m_1 = b_1^1 p + b_2^1 \frac{1}{p} \tag{5.1.34}$$

$$m_2 = b_3^1 - b_4^1 \frac{1}{p} \tag{5.1.35}$$

For New Model -II:

$$m_1 = b_1^2 p + b_2^2 \tag{5.1.36}$$

$$m_2 = b_3^2 \sqrt{p} - b_4^2 \frac{1}{\sqrt{p}} \tag{5.1.37}$$

where, $b_1^1 = 1$, $b_2^1 = \frac{A_2 - A_0 - a_2}{2A_3}$, $b_3^1 = \sqrt{\frac{a_2}{A_3}}$, $b_4^1 = \frac{A_1\sqrt{a_2}}{2(A_3)^{\frac{3}{2}}}$,

$b_1^2 = 1$, $b_2^2 = \frac{A_2 - A_0 - a_2}{2A_1}$, $b_3^2 = \sqrt{\frac{a_2}{A_1}}$, $b_4^2 = \frac{\sqrt{a_2}}{2(A_1)^{\frac{3}{2}}}(A_0 + \epsilon)$,

$A_0 = a_0,\ A_1 = 1 + a_0\tau,\ A_2 = \epsilon + a_0 + a_2,\ A_3 = \frac{1}{2}a_0\tau^2$

Now, by substituting m_1 and m_2 from equations (5.1.34)-(5.1.35) into the solutions given by equations (5.1.17) and (5.1.19)-(5.1.21) and using the expression

$$K_\nu(z) \approx \sqrt{\frac{\pi}{2z}} e^{-z} \left[1 + \frac{4\nu^2 - 1}{8z} + \frac{(4\nu^2 - 1)(4\nu^2 - 9)}{2(8z)^2} + ...\right]$$

we get the short-time approximated solutions for the distributions of displacement, temperature and stresses in the Laplace transform domain (r, p) for different problems 1-3 under New model-I and New model-II as follows:

Case of prolem-1

We find the following solutions in Laplace transfer domain:

In the context of New model-I:

$$\overline{u}\,(r,p) \simeq \frac{T_0 a_1}{r t_0} \sum_{i=1}^{2} e^{-m_i(r-1)}(1-e^{-pt_0}) \left[\frac{B_{i1}^1}{p^{i+2}} + \frac{B_{i2}^1}{p^{i+3}}\right] \tag{5.1.38}$$

$$\overline{\theta}\,(r,p) \simeq \frac{T_0}{r t_0} \sum_{i=1}^{2} e^{-m_i(r-1)}(1-e^{-pt_0}) \left[\frac{C_{i1}^1}{p^{6-2i}} + \frac{C_{i2}^1}{p^{6-i}}\right] \tag{5.1.39}$$

$$\overline{\sigma}_{rr}\,(r,p) \simeq \frac{T_0 a_1}{r t_0} \sum_{i=1}^{2} e^{-m_i(r-1)}(1-e^{-pt_0}) \left[\frac{D_{i1}^1}{p^2} + \frac{D_{i2}^1}{p^{i+2}}\right] \tag{5.1.40}$$

$$\overline{\sigma}_{\phi\phi}\,(r,p) \simeq \frac{T_0 a_1}{r t_0} \sum_{i=1}^{2} e^{-m_i(r-1)}(1-e^{-pt_0}) \left[\frac{E_{i1}^1}{p^2} + \frac{E_{i2}^1}{p^{i+2}}\right] \tag{5.1.41}$$

In the context of New model-II:

$$\overline{u}\,(r,p) \simeq \frac{T_0 a_1}{r t_0} \sum_{i=1}^{2} e^{-m_i(r-1)}(1-e^{-pt_0}) \left[\frac{B_{i1}^2}{p^{\frac{i+5}{2}}} + \frac{B_{i2}^2}{p^4}\right] \tag{5.1.42}$$

$$\overline{\theta}\,(r,p) \simeq \frac{T_0}{r t_0} \sum_{i=1}^{2} e^{-m_i(r-1)}(1-e^{-pt_0}) \left[\frac{C_{i1}^2}{p^{4-i}} - \frac{C_{i2}^2}{p^{5-i}}\right] \tag{5.1.43}$$

$$\overline{\sigma}_{rr}\,(r,p) \simeq \frac{T_0 a_1}{r t_0} \sum_{i=1}^{2} e^{-m_i(r-1)}(1-e^{-pt_0}) \left[\frac{D_{i1}^2}{p^2} + \frac{D_{i2}^2}{p^3}\right] \tag{5.1.44}$$

$$\overline{\sigma}_{\phi\phi}\,(r,p) \simeq \frac{T_0 a_1}{r t_0} \sum_{i=1}^{2} e^{-m_i(r-1)}(1-e^{-pt_0}) \left[\frac{E_{i1}^2}{p^2} + \frac{E_{i2}^2}{p^3}\right] \tag{5.1.45}$$

Case of problem-2

Here, we obtain the following solutions:

In the context of New model-I:

$$\overline{u}\,(r,p) \simeq \frac{T^* a_1}{r} \sum_{i=1}^{2} e^{-m_i(r-1)} \left[\frac{B_{i1}^{1'}}{p^{i+1}} + \frac{B_{i2}^{1'}}{p^{i+2}}\right] \tag{5.1.46}$$

$$\overline{\theta}(r,p) \simeq \frac{T^*}{r}\sum_{i=1}^{2} e^{-m_i(r-1)}\left[\frac{C_{i1}^{1'}}{p^{5-2i}}+\frac{C_{i2}^{1'}}{p^{5-i}}\right] \tag{5.1.47}$$

$$\overline{\sigma}_{rr}(r,p) \simeq \frac{T^*a_1}{r}\sum_{i=1}^{2} e^{-m_i(r-1)}\left[\frac{D_{i1}^{1'}}{p}+\frac{D_{i2}^{'}}{p^{i+1}}\right] \tag{5.1.48}$$

$$\overline{\sigma}_{\phi\phi}(r,p) \simeq \frac{T^*a_1}{r}\sum_{i=1}^{2} e^{-m_i(r-1)}\left[\frac{E_{i1}^{1'}}{p}+\frac{E_{i2}^{1'}}{p^{i+1}}\right] \tag{5.1.49}$$

In the context of New model-II:

$$\overline{u}(r,p) \simeq \frac{T^*a_1}{r}\sum_{i=1}^{2} e^{-m_i(r-1)}\left[\frac{B_{i1}^{2'}}{p^{\frac{i+3}{2}}}+\frac{B_{i2}^{2'}}{p^{3}}\right] \tag{5.1.50}$$

$$\overline{\theta}(r,p) \simeq \frac{T^*}{r}\sum_{i=1}^{2} e^{-m_i(r-1)}\left[\frac{C_{i1}^{2'}}{p^{3-i}}+\frac{C_{i2}^{2'}}{p^{4-i}}\right] \tag{5.1.51}$$

$$\overline{\sigma}_{rr}(r,p) \simeq \frac{T^*a_1}{r}\sum_{i=1}^{2} e^{-m_i(r-1)}\left[\frac{D_{i1}^{2'}}{p}+\frac{D_{i2}^{2'}}{p^{2}}\right] \tag{5.1.52}$$

$$\overline{\sigma}_{\phi\phi}(r,p) \simeq \frac{T^*a_1}{r}\sum_{i=1}^{2} e^{-m_i(r-1)}\left[\frac{E_{i1}^{2'}}{p}+\frac{E_{i2}^{2'}}{p^{2}}\right] \tag{5.1.53}$$

Case of problem-3

In this case, the solutions are derived as:

In the context of New model-I:

$$\overline{u}(r,p) \simeq \frac{\sigma^*}{r}\sum_{i=1}^{2} e^{-m_i(r-1)}\left[\frac{B_{i1}^{1''}}{p^{3i-1}}+\frac{B_{i2}^{1''}}{p^{3i}}\right] \tag{5.1.54}$$

$$\overline{\theta}(r,p) \simeq \frac{\sigma^*}{ra_1}\sum_{i=1}^{2} e^{-m_i(r-1)}\left[\frac{C_{i1}^{1''}}{p^{3}}+\frac{C_{i2}^{1''}}{p^{4}}\right] \tag{5.1.55}$$

$$\overline{\sigma}_{rr}(r,p) \simeq \frac{\sigma^*}{r}\sum_{i=1}^{2} e^{-m_i(r-1)}\left[\frac{D_{i1}^{1''}}{p^{2i-1}}+\frac{D_{i2}^{1''}}{p^{2i}}\right] \tag{5.1.56}$$

$$\overline{\sigma}_{\phi\phi}(r,p) \simeq \frac{\sigma^*}{r}\sum_{i=1}^{2} e^{-m_i(r-1)}\left[\frac{E_{i1}^{1''}}{p^{2i-1}} + \frac{E_{i2}^{1''}}{p^{2i}}\right] \tag{5.1.57}$$

In the context of New model-II:

$$\overline{u}(r,p) \simeq \frac{\sigma^*}{r}\sum_{i=1}^{2} e^{-m_i(r-1)}\left[\frac{B_{i1}^{2''}}{p^{\frac{3i+1}{2}}} + \frac{B_{i2}^{2''}}{p^{i+2}}\right] \tag{5.1.58}$$

$$\overline{\theta}(r,p) \simeq \frac{\sigma^*}{ra_1}\sum_{i=1}^{2} e^{-m_i(r-1)}\left[\frac{C_{i1}^{2''}}{p^2} + \frac{C_{i2}^{2''}}{p^3}\right] \tag{5.1.59}$$

$$\overline{\sigma}_{rr}(r,p) \simeq \frac{\sigma^*}{r}\sum_{i=1}^{2} e^{-m_i(r-1)}\left[\frac{D_{i1}^{2''}}{p^i} + \frac{D_{i2}^{2''}}{p^{i+1}}\right] \tag{5.1.60}$$

$$\overline{\sigma}_{\phi\phi}(r,p) \simeq \frac{\sigma^*}{r}\sum_{i=1}^{2} e^{-m_i(r-1)}\left[\frac{E_{i1}^{2''}}{p^i} + \frac{E_{i2}^{2''}}{p^{i+1}}\right] \tag{5.1.61}$$

where different notations used in solutions given by (5.1.38)-(5.1.61), are mentioned in the following expressions:

$B_{11}^1 = B_{11}^{1'} = D_{21}^1 = D_{21}^{1'} = D_{11}^{1''} = E_{21}^1 = E_{21}^{1'} = -1,$

$C_{21}^1 = C_{21}^{1'} = D_{11}^1 = D_{11}^{1'} = B_{11}^{1''} = 1,$

$B_{12}^1 = B_{12}^{1'} = -\frac{1-2r+2r\lambda_1}{r}$, $B_{21}^1 = B_{21}^{1'} = \frac{1+b_3^1 r}{r}$, $B_{12}^{1''} = \frac{1-2r+2r\lambda_1}{r}$,

$B_{22}^1 = B_{22}^{1'} = -b_4^1, C_{11}^1 = C_{11}^{1'} = C_{21}^{1''} = C_{22}^{1'} = D_{21}^{1''} = 2b_2^1,$

$C_{12}^1 = C_{12}^{1'} = C_{22}^{1''} = D_{22}^{1''} = -4b_2^1(1-\lambda_1),$

$E_{22}^{1''} = C_{12}^{1''} = 4b_2^1(1-\lambda_1)$, $E_{21}^{1''} = C_{11}^{1''} = C_{22}^1 = -2b_2^1,$

$D_{12}^1 = D_{12}^{1'} = D_{12}^{1''} = \frac{2(1-\lambda_1)(r-1)}{r}$, $E_{12}^{1''} = -\frac{2(1+2r\lambda_1)(\lambda_1-1)}{r}$,

$D_{22}^1 = D_{22}^{1'} = -\frac{2+2b_3^1 r-2b_2^1 r^2+(b_3^1)^2 r^2-2\lambda_1-2b_3^1 r\lambda_1}{r^2}$, $E_{11}^1 = \lambda_1,$

$E_{12}^{1'} = \frac{\lambda_1-2r\lambda_1+2r\lambda_1^2-1}{r},,$ $E_{22}^1 = E_{22}^{1'} = -\frac{b_3^1 r^2\lambda_1+b_3^1 r\lambda_1+\lambda_1-2b_2^1 r-b_3^1 r-1}{r^2},$

$B_{21}^{1''} = \frac{2b_2^1(1+b_3^1 r)}{r}$, $B_{22}^{1''} = \frac{2b_2^1(-2-2b_3^1 r-b_4^1 r+2\lambda_1+2b_3^1 r\lambda_1)}{r}$, $E''^1_{11} = -\lambda_1,$

$B_{11}^2 = B_{11}^{2'} = B_{11}^{2''} = D_{21}^2 = D_{11}^{2''} = E_{21}^2 = E_{21}^{2'} = D_{21}^{2'} = -1,$

$D_{11}^2 = D_{11}^{2'} = C_{21}^2 = C_{21}^{2'} = 1$, $B_{12}^2 = B_{12}^{2'} = \frac{-(1-2r-rb_2^2+rb_3^2+2\lambda_1)}{r}$,

$B_{21}^2 = B_{21}^{2'} = b_3^2$, $B_{22}^2 = B_{22}^{2'} = \frac{1}{r}$,

$C_{12}^2 = -b_2^2(-4-3b_2^2+2(b_3^2)^2+4\lambda_1)$, $E_{11}^2 = E_{11}^{2'} = \lambda_1$, $E_{11}^{2''} = -\lambda_1$,

$D_{12}^2 = D_{12}^{2'} = \frac{1}{r}(2-2r-2rb_2^2+(rb_3^2)^2-2\lambda_1+2r\lambda_1)$,

$D_{22}^2 = D_{22}^{2'} = -(-2b_2^2+(b_3^2)^2)$, $C_{22}^2 = C_{22}^{2'} = C_{11}^{2''} = D_{21}^{2''} = E_{21}^{2''} = -2b_2^2$,

$E_{12}^2 = E_{12}^{2'} = \frac{1}{r}(-1-2rb_2^2+\lambda_1-2r\lambda_1+r\lambda_1(b_3^2)^2+2r\lambda_1^2)$, $E_{22}^2 = -\frac{1}{2b_3^2}$,

$C_{12}^{2'\cdot} = b_2^2(-4-3b_2^2+(b_3^2)^2+4\lambda_1)$, $E_{22}^{2'} = -4b_2^2b_3^2+(b_3^2)^2\lambda_1$,

$B_{12}^{2''} = -\frac{1}{r}(-1+2r+rb_2^2-2r\lambda_1)$, $B_{21}^{2''} = -2b_2^2b_3^2$, $B_{22}^{2''} = \frac{1}{r}(-2b_2^2)$,

$C_{12}^{2''\cdot} = C_{22}^{2''\cdot} = b_2^2(4+3b_2^2-4\lambda_1)$, $D_{12}^{2''} = \frac{2}{r}(-1+r+rb_2^2+\lambda_1-r\lambda_1)$,

$D_{22}^{2''} = (4+3b_2^2-2(b_3^2)^2-4\lambda_1)$, $E_{12}^2 = \frac{1}{r}(-1-2rb_2^2+\lambda_1-2r\lambda_1+2r\lambda_1^2)$,

$E_{22}^{2''} = 4+3b_2^2-4\lambda_1-2(b_3^2)^2\lambda_1$.

5.1.7 Solutions in the Physical Domain

Now, we use inversion of the Laplace transform for the above obtained solutions. For this, we use the convolution theorem and the formulae listed below (1973).

$$L^{-1}\left[\frac{e^{-\frac{a}{p}}}{p^{\nu+1}}\right] = \left(\frac{t}{a}\right)^{\frac{\nu}{2}} J_\nu(2\sqrt{at}), \quad Re(\nu) > -1,\ a > 0$$

$$L^{-1}\left[\frac{e^{\frac{a}{p}}}{p^{\nu+1}}\right] = \left(\frac{t}{a}\right)^{\frac{\nu}{2}} I_\nu(2\sqrt{at}), \quad Re(\nu) > -1,\ a > 0$$

$$L^{-1}\left[\frac{e^{-a\sqrt{p}}}{p^{\frac{\nu}{2}+1}}\right] = (4t)^{\frac{\nu}{2}}\, \boldsymbol{i}^\nu \mathrm{erfc}(\frac{a}{2\sqrt{t}}), \quad \nu = 0, 1, 2...$$

Here, J_ν, I_ν are the Bessel and modified Bessel functions of order ν and of the first kind, and $\boldsymbol{i}^n\mathrm{erfc}(x)$ is complementary error function of n$^{\text{th}}$ order defined by

$\boldsymbol{i}^n\mathrm{erfc}(x) = \int_x^\infty \boldsymbol{i}^{n-1}\mathrm{erfc}(u)du, \quad n = 1, 2, 3...$

with $\operatorname{erfc}(x) = \frac{2}{\sqrt{\pi}} \int_x^\infty \mathrm{e}^{-\mathrm{t}^2} dt$.

Now, by taking inverse Laplace transform of equations (5.1.38)-(5.1.61), we get the approximated analytical solutions for the distributions of displacement, temperature and stresses in space-time domain in the following forms:

For problem-1

Solutions in the context of New model- I:

$$
\begin{aligned}
u(r,t) = \frac{T_0 a_1}{r t_0} \sum_{i=1}^{2} \Bigg[& B_{1i}^1 \left(\frac{t - b_1^1 r_1}{b_2^1 r_1} \right)^{i+1/2} J_{i+1} \left(2\sqrt{b_2^1 r_1 (t - b_1^1 r_1)} \right) H(t - b_1^1 r_1) \\
& + B_{2i}^1 e^{-b_3^1 r_1} \left(\frac{t}{b_4^1 r_1} \right)^{\frac{2+i}{2}} I_{2+i} \left(2\sqrt{b_4^1 r_1 t} \right) \Bigg] \\
& - \frac{T_0 a_1}{r t_0} \sum_{i=1}^{2} \Bigg[B_{1i}^1 \left(\frac{t - b_1^1 r_1 - t_0}{b_2^1 r_1} \right)^{i+1/2} J_{i+1} \left(2\sqrt{b_2^1 r_1 (t - b_1^1 r_1 - t_0)} \right) H(t - b_1^1 r_1 - t_0) \\
& + B_{2i}^1 e^{-b_3^1 r_1} \left(\frac{t - t_0}{b_4^1 r_1} \right)^{\frac{2+i}{2}} I_{2+i} \left(2\sqrt{b_4^1 r_1 (t - t_0)} \right) H(t - t_0) \Bigg]
\end{aligned} \tag{5.1.62}
$$

$$
\begin{aligned}
\theta(r,t) = \frac{T_0}{r t_0} \sum_{i=1}^{2} \Bigg[& C_{1i}^1 \left(\frac{t - b_1^1 r_1}{b_2'} \right)^{(i+2)/2} J_{i+2} \left(2\sqrt{b_2^1 r_1 (t - b_1^1 r_1)} \right) H(t - b_1^1 r_1) \\
& + C_{2i}^1 e^{-b_3^1 r_1} \left(\frac{t}{b_4^1 r_1} \right)^{(2i-1)/2} I_{2i-1} \left(2\sqrt{b_4^1 r_1 t} \right) \Bigg] \\
& - \frac{T_0}{r t_0} \sum_{i=1}^{2} \Bigg[C_{1i}^1 \left(\frac{t - b_1^1 r_1 - t_0}{b_2'} \right)^{(i+2)/2} J_{i+2} \left(2\sqrt{b_2^1 r_1 (t - b_1^1 r_1 - t_0)} \right) H(t - b_1^1 r_1 - t_0) \\
& + C_{2i}^1 e^{-b_3^1 r_1} \left(\frac{t - t_0}{b_4^1 r_1} \right)^{(2i-1)/2} I_{2i-1} \left(2\sqrt{b_4^1 r_1 (t - t_0)} \right) H(t - t_0) \Bigg]
\end{aligned} \tag{5.1.63}
$$

$$
\begin{aligned}
\sigma_{rr}(r,t) = \frac{T_0 a_1}{r t_0} \sum_{i=1}^{2} \Bigg[& D_{1i}^1 \left(\frac{t - b_1^1 r_1}{b_2'} \right)^{i/2} J_i \left(2\sqrt{b_2^1 r_1 (t - b_1^1 r_1)} \right) H(t - b_1^1 r_1) \\
& + D_{2i}^1 e^{-b_3^1 r_1} \left(\frac{t}{b_4^1 r_1} \right)^{(2i-1)/2} I_{2i-1} \left(2\sqrt{b_4^1 r_1 t} \right) \Bigg] \\
& - \frac{T_0 a_1}{r t_0} \sum_{i=1}^{2} \Bigg[D_{1i}^1 \left(\frac{t - b_1^1 r_1 - t_0}{b_2'} \right)^{i/2} J_i \left(2\sqrt{b_2^1 r_1 (t - b_1^1 r_1 - t_0)} \right) H(t - b_1^1 r_1 - t_0) \\
& + D_{2i}^1 e^{-b_3^1 r_1} \left(\frac{t - t_0}{b_4^1 r_1} \right)^{(2i-1)/2} I_{2i-1} \left(2\sqrt{b_4^1 r_1 (t - t_0)} \right) H(t - t_0) \Bigg]
\end{aligned} \tag{5.1.64}
$$

$$\sigma_{\phi\phi}(r,t) = \frac{T_0 a_1}{r t_0}\sum_{i=1}^{2}\left[E_{1i}^{1}\left(\frac{t-b_1^1 r_1}{b_2^1 r_1}\right)^{i/2} J_i\left(2\sqrt{b_2^1 r_1 (t-b_1^1 r_1)}\right) H(t-b_1^1 r_1)\right.$$
$$\left. + E_{2i}^{1} e^{-b_3^1 r_1}\left(\frac{t}{b_4^1 r_1}\right)^{(2i-1)/2} I_{2i-1}\left(2\sqrt{b_4^1 r_1 t}\right)\right]$$
$$- \frac{T_0 a_1}{r t_0}\sum_{i=1}^{2}\left[E_{1i}^{1}\left(\frac{t-b_1^1 r_1 - t_0}{b_2^1 r_1}\right)^{i/2} J_i\left(2\sqrt{b_2^1 r_1 (t-b_1^1 r_1 - t_0)}\right) H(t-b_1^1 r_1 - t_0)\right.$$
$$\left. + E_{2i}^{1} e^{-b_3^1 r_1}\left(\frac{t-t_0}{b_4^1 r_1}\right)^{(2i-1)/2} I_{2i-1}\left(2\sqrt{b_4^1 r_1 (t-t_0)}\right) H(t-t_0)\right] \tag{5.1.65}$$

Solutions in the context of New model II:

$$u(r,t) = \frac{T_0 a_1}{r t_0}\sum_{i=1}^{2} e^{-b_2^2 r_1}\left[B_{1i}^{1}\frac{(t-b_1^2 r_1)^{i+1}}{4i-2}H(t-b_1^2 r_1) - B_{1i}^{2}H(t-b_1^2 r_1 - t_0)\frac{(t-b_1^2 r_1 - t_0)^{i+1}}{4i-2}\right]$$
$$+ \frac{T_0 a_1}{r t_0}\sum_{i=1}^{2}\left[B_{2i}^{2}(4t)^{\frac{i+2}{2}}\boldsymbol{i}^{i+4}\mathrm{erfc}(\frac{b_3^2 r_1}{2\sqrt{t}}) - B_{2i}^{2}(4t)^{\frac{i+2}{2}}\boldsymbol{i}^{i+4}\mathrm{erfc}(\frac{b_3^2 r_1}{2\sqrt{t-t_0}})H(t-t_0)\right] \tag{5.1.66}$$

$$\theta(r,t) = \frac{T_0}{r t_0}\sum_{i=1}^{2} e^{-b_2^2 r_1}\left[C_{1i}^{2}\frac{(t-b_1^2 r_1)^{i+1}}{4i-2}H(t-b_1^2 r_1) - C_{1i}^{2}H(t-b_1^2 r_1 - t_0)\frac{(t-b_1^2 r_1 - t_0)^{i+1}}{4i-2}\right]$$
$$+ \frac{T_0}{r t_0}\sum_{i=1}^{2}\left[C_{2i}^{2}(4t)^{i}\boldsymbol{i}^{2i}\mathrm{erfc}(\frac{b_3^2 r_1}{2\sqrt{t}}) - C_{2i}^{2}(4(t-t_0))^{i}\boldsymbol{i}^{2i}\mathrm{erfc}(\frac{b_3^2 r_1}{2\sqrt{t-t_0}})H(t-t_0)\right] \tag{5.1.67}$$

$$\sigma_{rr}(r,t) = \frac{T_0 a_1}{r t_0}\sum_{i=1}^{2} e^{-b_2^2 r_1}\left[D_{1i}^{2}\frac{(t-b_1^2 r_1)^{i}}{i}H(t-b_1^2 r_1) - D_{1i}^{2}H(t-b_1^2 r_1 - t_0)\frac{(t-b_1^2 r_1 - t_0)^{i}}{i}\right]$$
$$+ \frac{T_0 a_1}{r t_0}\sum_{i=1}^{2}\left[D_{2i}^{2}(4t)^{i}\boldsymbol{i}^{2i}\mathrm{erfc}(\frac{b_3^2 r_1}{2\sqrt{t}}) - D_{2i}^{2}(4(t-t_0))^{i}\boldsymbol{i}^{2i}\mathrm{erfc}(\frac{b_3^2 r_1}{2\sqrt{t-t_0}})H(t-t_0)\right] \tag{5.1.68}$$

$$\sigma_{\phi\phi}(r,t) = \frac{T_0 a_1}{r t_0}\sum_{i=1}^{2} e^{-b_2^2 r_1}\left[E_{1i}^{2}\frac{(t-b_1^2 r_1)^{i}}{i}H(t-b_1^{2'}) - E_{1i}^{2}H(t-b_1^2 r_1 - t_0)\frac{(t-b_1^2 r_1 - t_0)^{i}}{i}\right]$$
$$+ \frac{T_0 a_1}{r t_0}\sum_{i=1}^{2}\left[E_{2i}^{2}(4t)^{i}\boldsymbol{i}^{2i}\mathrm{erfc}(\frac{b_3^2 r_1}{2\sqrt{t}}) - E_{2i}^{2}(4(t-t_0))^{i}\boldsymbol{i}^{2i}\mathrm{erfc}(\frac{b_3^2 r_1}{2\sqrt{t-t_0}})H(t-t_0)\right] \tag{5.1.69}$$

For problem-2

Solutions in the context of New model-I:

$$u\left(r,t\right)=\frac{T^{*}a_{1}}{r}\Bigg[\sum_{i=1}^{2}-B_{1i}^{1'}\left(\frac{t-b_{1}^{1}r_{1}}{b_{2}^{1}r_{1}}\right)^{\frac{i}{2}}J_{i}\left(2\sqrt{b_{2}^{1}r_{1}(t-b_{1}^{1}r_{1})}\right)H(t-b_{1}^{1}r_{1})$$
$$+\sum_{i=1}^{2}B_{2i}^{1'}e^{-b_{3}^{1}r_{1}}\left(\frac{t}{b_{4}^{1}r_{1}}\right)^{\frac{i+1}{2}}I_{i+1}\left(2\sqrt{b_{4}^{1}r_{1}t}\right)\Bigg] \tag{5.1.70}$$

$$\theta\left(r,t\right)=\frac{T^{*}}{r}\Bigg[\sum_{i=1}^{2}C_{1i}^{1'}\left(\frac{t-b_{1}^{1}r_{1}}{b_{2}^{1}r_{1}}\right)^{(i+1)/2}J_{i+1}\left(2\sqrt{b_{2}^{1}r_{1}(t-b_{1}^{1}r_{1})}\right)H(t-b_{1}^{1}r_{1})$$
$$+\sum_{i=1}^{2}(-1)^{i+1}C_{2i}^{1'}e^{-b_{3}^{1}r_{1}}\left(\frac{t}{b_{4}^{1}r_{1}}\right)^{2i-2/2}I_{2i-2}\left(2\sqrt{b_{4}^{1}r_{1}t}\right)\Bigg] \tag{5.1.71}$$

$$\sigma_{rr}\left(r,t\right)=\frac{T^{*}a_{1}}{r}\Bigg[\sum_{i=1}^{2}D_{1i}^{1'}\left(\frac{t-b_{1}^{1}r_{1}}{b_{2}^{1}r_{1}}\right)^{(i-1)/2}J_{i-1}\left(2\sqrt{b_{2}^{1}r_{1}(t-b_{1}^{1}r_{1})}\right)H(t-b_{1}^{1}r_{1})$$
$$+\sum_{i=1}^{2}D_{2i}^{1'}e^{-b_{3}^{1}r_{1}}\left(\frac{t}{b_{4}^{1}r_{1}}\right)^{(2i-2)/2}I_{2i-2}\left(2\sqrt{b_{4}^{1}r_{1}t}\right)\Bigg] \tag{5.1.72}$$

$$\sigma_{\phi\phi}\left(r,t\right)=\frac{T^{*}a_{1}}{r}\Bigg[\sum_{i=1}^{2}E_{1i}^{1'}\left(\frac{t-b_{1}^{1}r_{1}}{b_{2}^{1}r_{1}}\right)^{(i-1)/2}J_{i-1}\left(2\sqrt{b_{2}^{1}r_{1}(t-b_{1}^{1}r_{1})}\right)H(t-b_{1}^{1}r_{1})$$
$$+\sum_{i=1}^{2}E_{2i}^{1'}e^{-b_{3}^{1}r_{1}}\left(\frac{t}{b_{4}^{1}r_{1}}\right)^{(2i-2)/2}I_{2i-2}\left(2\sqrt{b_{4}^{1}r_{1}t}\right)\Bigg] \tag{5.1.73}$$

Solutions in the context of New model-II:

$$u\left(r,t\right)=\frac{T^{*}a_{1}}{r}\sum_{i=1}^{2}\left[e^{-b_{2}^{2}r_{1}}\left\{B_{1i}^{2'}\frac{(t-b_{1}^{2}r_{1})^{i}}{i}H(t-b_{1}^{2}r_{1})\right\}+\left\{B_{2i}^{2'}(4t)^{\frac{i+2}{2}}\boldsymbol{i}^{i+2}\mathrm{erfc}(\frac{b_{3}^{2}r_{1}}{2\sqrt{t}})\right\}\right] \tag{5.1.74}$$

$$\theta\left(r,t\right)=\frac{T^{*}}{r}\sum_{i=1}^{2}\left[e^{-b_{2}^{2}r_{1}}\left\{C_{1i}^{2'}\frac{(t-b_{1}^{2}r_{1})^{i}}{i}H(t-b_{1}^{2}r_{1})\right\}+\left\{C_{2i}^{2'}(4t)^{i-1}\boldsymbol{i}^{2i-2}\mathrm{erfc}(\frac{b_{3}^{2}r_{1}}{2\sqrt{t}})\right\}\right] \tag{5.1.75}$$

$$\sigma_{rr}\left(r,t\right)=\frac{T^{*}a_{1}}{r}\sum_{i=1}^{2}\left[e^{-b_{2}^{2}r_{1}}\left\{D_{1i}^{2'}(t-b_{1}^{2}r_{1})^{i-1}H(t-b_{1}^{2}r_{1})\right\}+\left\{D_{2i}^{2'}(4t)^{i-1}\boldsymbol{i}^{2i-2}\mathrm{erfc}(\frac{b_{3}^{2}r_{1}}{2\sqrt{t}})\right\}\right] \tag{5.1.76}$$

$$\sigma_{\phi\phi}(r,t)=\frac{T^{*}a_1}{r}\sum_{i=1}^{2}\left[e^{-b_2^2r_1}\left\{E_{1i}^{2'}(t-b_1^2r_1)^{i-1}H(t-b_1^2r_1)\right\}+\left\{E_{2i}^{2'}(4t)^{i-1}\boldsymbol{i}^{2i-2}\mathrm{erfc}(\frac{b_3^2r_1}{2\sqrt{t}})\right\}\right] \tag{5.1.77}$$

For problem-3

Solutions in the context of New model-I:

$$u(r,t)=\frac{\sigma^{*}}{r}\Bigg[\sum_{i=1}^{2}B_{1i}^{1''}\left(\frac{t-b_1^1r_1}{b_2^1r_1}\right)^{\frac{i}{2}}J_i\left(2\sqrt{b_2^1r_1(t-b_1^1r_1)}\right)H(t-b_1^1r_1)$$
$$+\sum_{i=1}^{2}B_{2i}^{1''}e^{-b_3^1r_1}\left(\frac{t}{b_4^1r_1}\right)^{\frac{i+3}{2}}I_{i+3}\left(2\sqrt{b_4^1r_1(t)}\right)\Bigg] \tag{5.1.78}$$

$$\theta(r,t)=\frac{\sigma^{*}}{ra_1}\Bigg[\sum_{i=1}^{2}C_{1i}^{1''}\left(\frac{t-b_1^1r_1}{b_2^1r_1}\right)^{(i+1)/2}J_{i+1}\left(2\sqrt{b_2^1r_1(t-b_1^1r_1)}\right)H(t-b_1^1r_1)$$
$$+\sum_{i=1}^{2}C_{2i}^{1''}e^{-b_3^1r_1}\left(\frac{t}{b_4^1r_1}\right)^{(i+1)/2}I_{i+1}\left(2\sqrt{b_4^1r_1t}\right)\Bigg] \tag{5.1.79}$$

$$\sigma_{rr}(r,t)=\frac{\sigma^{*}}{r}\Bigg[\sum_{i=1}^{2}D_{1i}^{1''}\left(\frac{t-b_1^1r_1}{b_2^1r_1}\right)^{(i-1)/2}J_{i-1}\left(2\sqrt{b_2^1r_1(t-b_1^1r_1)}\right)H(t-b_1^1r_1)$$
$$+\sum_{i=1}^{2}D_{2i}^{1''}e^{-b_3^1r_1}\left(\frac{t}{b_4^1r_1}\right)^{(i+1)/2}I_{i+1}\left(2\sqrt{b_4^1r_1t}\right)\Bigg] \tag{5.1.80}$$

$$\sigma_{\phi\phi}(r,t)=\frac{\sigma^{*}}{r}\Bigg[\sum_{i=1}^{2}E_{1i}^{1''}\left(\frac{t-b_1^1r_1}{b_2^1r_1}\right)^{(i-1)/2}J_{i-1}\left(2\sqrt{b_2^1r_1(t-b_1^1r_1)}\right)H(t-b_1^1r_1)$$
$$+\sum_{i=1}^{2}E_{2i}^{1''}e^{-b_3^1r_1}\left(\frac{t}{b_4^1r_1}\right)^{(i+1)/2}I_{i+1}\left(2\sqrt{b_4^1r_1t}\right)\Bigg] \tag{5.1.81}$$

Solutions in the context of New model-II:

$$u(r,t)=\frac{\sigma^{*}}{r}\sum_{i=1}^{2}\left[e^{-b_2^2r_1}\left\{B_{1i}^{2''}\frac{(t-b_1^2r_1)^{i}}{i}H(t-b_1^{2'})\right\}+\left\{B_{2i}^{2''}(4t)^{\frac{3i}{2}}\boldsymbol{i}^{3i}\mathrm{erfc}(\frac{b_3^2r_1}{2\sqrt{t}})\right\}\right] \tag{5.1.82}$$

$$\theta(r,t)=\frac{\sigma^{*}}{ra_1}\sum_{i=1}^{2}\left[e^{-b_2^2r_1}\left\{C_{1i}^{2''}\frac{(t-b_1^2r_1)^{i}}{i}H(t-b_1^2r_1)\right\}+\left\{C_{2i}^{2''}(4t)^{i}\boldsymbol{i}^{2i}\mathrm{erfc}(\frac{b_3^2r_1}{2\sqrt{t}})\right\}\right] \tag{5.1.83}$$

$$\sigma_{rr}\left(r,t\right)=\frac{\sigma^{*}}{r}\sum_{i=1}^{2}\left[e^{-b_{2}^{2}r_{1}}\left\{D_{1i}^{2''}(t-b_{1}^{2}r_{1})^{i-1}H(t-b_{1}^{2}r_{1})\right\}+\left\{D_{2i}^{2''}(4t)^{i}\boldsymbol{i}^{2i}\mathrm{erfc}(\frac{b_{3}^{2}r_{1}}{2\sqrt{t}})\right\}\right] \tag{5.1.84}$$

$$\sigma_{\phi\phi}\left(r,t\right)=\frac{\sigma^{*}}{r}\sum_{i=1}^{2}\left[e^{-b_{2}^{2}r_{1}}\left\{E_{1i}^{2''}(t-b_{1}^{2}r_{1})^{1-i}H(t-b_{1}^{2}r_{1})\right\}+\left\{E_{2i}^{2''}(4t)^{i}\boldsymbol{i}^{2i}\mathrm{erfc}(\frac{b_{3}^{2}r_{1}}{2\sqrt{t}}\right\}\right] \tag{5.1.85}$$

where, $r_1 = (r-1)$.

5.1.8 Analysis of Analytical Results

From the short-time approximated solutions obtained for the **case of problem-1**, i.e., when the boundary of the spherical cavity is subjected to a ramp-type heating, we observe that the distributions of displacement, temperature and stresses for the case of New model-I consist of four different terms. The terms involving $H(t-b_1^1 r_1)$ and $H(t-b_1^1 r_1-t_0)$ corresponds to a wave propagating with nondimensional finite speeds $\frac{1}{b_1^1}$ and $\frac{1}{b_1^1-t_0}$, respectively. These waves can be identified as predominantly elastic waves propagating with different phases. The expressions, given by equations (5.1.62)–(5.1.65) reveal that under New model-I, the modified elastic wave propagates without any attenuation. This is a distinct feature predicted by the theory and it has a similarity with the case of GN-II model. Furthermore, we note that the speed of elastic waves do not depend on the delay parameter or any material parameters. The second and fourth part of the solutions of the field variables do not indicate to be a contribution of a wave. On the contrary, it is diffusive in nature indicating an exponential decay with distance with an attenuating coefficient b_3^1. This represents that under this present model, the thermal wave do not propagate with finite wave speed like other generalized thermoelasticity theories, namely Lord-Shulman model, Green-Lindsay model, GN-II model, dual-phase-lag model, or three-phase-lag model. Furthermore, we note that the solutions for all fields give by equations (5.1.62) - (5.1.65) are continuous in nature.

In the context of the New model-II from equations (5.1.66) - (5.1.69), we observe that

solutions for the distribution of displacement, temperature and stresses also consist of four different contributions. As in the previous case, the terms involving $H(t - b_1^2 r_1)$ and $H(t - b_1^2 r_1 - t_0)$ correspond to two waves (modified elastic waves) propagating with nondimensional finite speeds $\frac{1}{b_1^2}$ and $\frac{1}{b_1^2 - t_0}$. Unlike New model-I, this New model-II predicts that elastic waves decay exponentially with an attenuating coefficient b_2^2. The wave speed in the case of model-I and model-II exactly same and do not depend on any material parameters. However, the attenuation coefficient of modified elastic waves in the case of New model-II depend on the delay time as well as on the material parameters. The other parts of solutions are diffusive in nature due to the damping term. The solutions of all fields are continuous in nature in this case too.

From the solutions given by equations (5.1.70)–(5.1.77) **in case of problem-2**, we observe that as in problem-1, each of the distributions of temperature, displacement, and stress consists of two main parts. In the first part, the terms involving $H(t - b_1^2 r_1)$ and $H(t - b_1^2 r_1)$ correspond to pre-dominantly elastic waves propagating with non dimensional finite speeds of $\frac{1}{b_1^1}$ and $\frac{1}{b_1^2}$, for New model-I and New model- II, respectively. The wave speeds are same as in case of problem-1. In view of the expressions represented by equations (5.1.70)–(5.1.73) under New model- I, we note that the elastic wave propagates without any attenuation, whereas in the solutions represented by equations (5.1.74)-(5.1.77) under New model- II, elastic wave propagates with an attenuation coefficient b_2^2 that depends upon the delay time and material parameters. The second part of the solutions given by equations (5.1.70)-(5.1.77) show that the field variables do not indicate to be a contribution of a wave. Instead of that, it is diffusive in nature. It indicates an exponential decay with distance with an attenuating coefficient b_3^1 for New model- I. Furthermore, we note that the solutions for temperature and displacement are continuous in nature for both the models. However, the analytical results, given by equations (5.1.72)-(5.1.73) for New model- I show that stress distributions suffer from the finite discontinuity at elastic wave front. The finite jumps are obtained as follows:

$$\sigma_{rr}\big|_{r_1=\frac{t}{b_1^1}} = \sigma_{rr}\big|_{r_1=\frac{t^+}{b_1^1}} - \sigma_{rr}\big|_{r_1=\frac{t^-}{b_1^1}} = D_{11}^{1'}\frac{T^* a_1}{r}$$

$$\sigma_{\phi\phi}|_{r_1=\frac{t}{b_1^1}} = \sigma_{\phi\phi}|_{r_1=\frac{t^+}{b_1^1}} - \sigma_{\phi\phi}|_{r_1=\frac{t^-}{b_1^1}} = E_{11}^{1'}\frac{T^*a_1}{r}$$

Like the solutions for New model-I, in the solutions of radial stress and circumferential stress distributions given by equations (5.1.76)-(5.1.77), we observe similar characteristic for New model- II. In this case, the finite jumps at the elastic wavefront are found out as follows:

$$\sigma_{rr}|_{r_1=\frac{t}{b_1^2}} = \sigma_{rr}|_{r_1=\frac{t^+}{b_1^2}} - \sigma_{rr}|_{r_1=\frac{t^-}{b_1^2}} = D_{11}^{2'}e^{-\frac{b_2^2 t}{b_1^1}}\frac{T^*a_1}{r}$$

$$\sigma_{\phi\phi}|_{r_1=\frac{t}{b_1^2}} = \sigma_{\phi\phi}|_{r_1=\frac{t^+}{b_1^2}} - \sigma_{\phi\phi}|_{r_1=\frac{t^-}{b_1^2}} = E_{11}^{2'}e^{-\frac{b_2^2 t}{b_1^1}}\frac{T^*a_1}{r}$$

In case of problem- 3, we note that the solutions for the field variables have two main parts, like the case of problem-II. The first part in each solution represents elastic waves propagating with the speed $\frac{1}{b_1^1}$ and it propagate without any attenuation in the case of New model-I, whereas New model-II predicts that the predominating elastic waves have speed $\frac{1}{b_1^2}$ and an attenuation coefficient b_2^2. The second parts of the solutions are of diffusive nature which is because of the parabolic nature of heat transport equation in this case. As in the case of problem-2, in the present case also the radial stress and circumferential stress distributions show discontinuities with finite jumps at the elastic wave front under both the models i.e. under New model- I and New model -II.

5.1.9 Numerical Results and Discussion

In the previous section, we obtained short-time approximated analytical results for the physical fields and we noted some significant differences in the natures of solutions. In this section, we make an attempt to find the numerical solutions of the problem by carrying out the Laplace inversions for temperature, displacement, radial stress and shear stress with the help of programming in mathematical software and by employing a suitable numerical method of Laplace inversion. We employ here the method given

by Honig and Hirdes (1984), which is based on the method proposed by Durbin (1973) for the Laplace inversion. The method of numerical inversion is appended at the end at this section (see Appendix A).

We assume that the spherical cavity is made of copper material and the physical data for which are taken as below (Sherief and Saleh (2005)):

$\lambda = 7.76\times10^{10}\ Nm^{-2}$, $\mu = 3.86\times10^{10}\ Nm^{-2}$, $\alpha_t = 1.78\times10^{-5}\ K^{-1}$, $\eta = 8886.73\ sm^{-2}$, $c_E = 383.1\ JKg^{-1}K^{-1}$, $\rho = 8954\ Kg\ m^{-3}$, $T_0 = 293K$.

In order to analyze the solutions for non-dimensional temperature, displacement, radial stress and tangential stress in space-time domain inside the spherical cavity, the results under three different problems are displayed in Figs. 5.1.1(a, b, c, d)-5.1.3(a, b, c, d). We have also consider the case under GN-III model by assuming $\tau = 0$ for the solution of the present problem and compared our results with the corresponding results of GN-III model. In each figure, we plotted the graphs for the fields at two different times, $t = 0.1$, $t = 0.3$ and for three different generalized thermoelastic models namely, New model-I, New model-II and GN-III model. Specially, we aim to understand the effect of thermal relaxation parameter, τ, on the solutions at various times and highlight the specific features of the recent heat conduction model. The important facts under various cases of prescribed boundary conditions arising out from our investigation are highlighted as follows:

Discussion on results of Problem-1:

Figures 5.1.1(a, b, c, d) show the variations in field variables u, θ, σ_{rr} and $\sigma_{\phi\phi}$ with respect to radial distance r for the one of problem-1. From the graphs, it is clear that at any particular time there is no prominent difference in the solutions of the field variables under three models in the problem when the boundary is subjected to a ramp-type heating. This implies that there is not much effect of delay parameter, τ on the distributions of the field variables and the recent model predicts similar results like the Green-Naghdi model of thermoelasticity. However, the region of influence for each

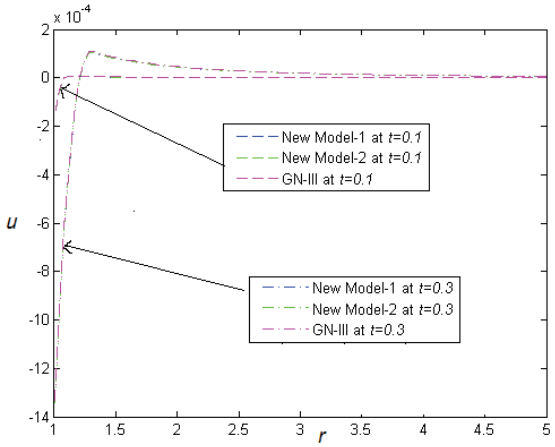

Fig. 5.1.1(a) : Variation of u vs. r for different values of t under Problem-I.

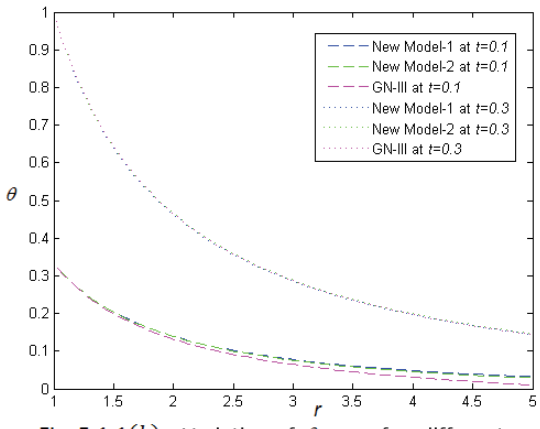

Fig. 5.1.1(b) : Variation of θ vs. r for different values of t under Problem-I.

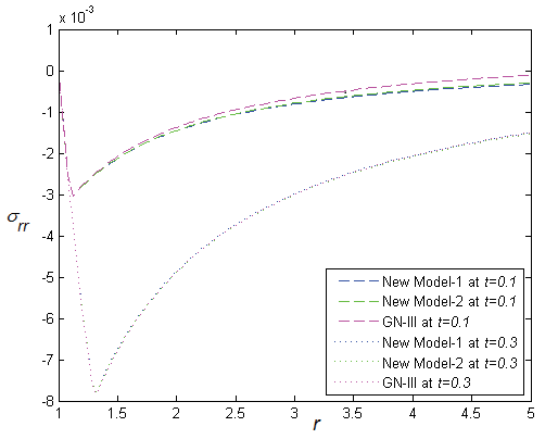

Fig. 5.1.1(c) : Variation of σ_{rr} vs. r for different values of t under Problem-I.

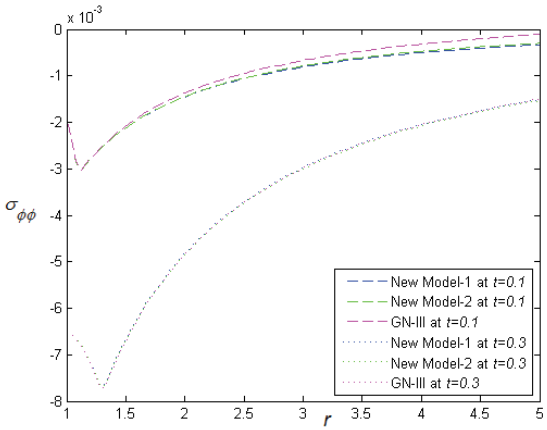

Fig. 5.1.1(d) : Variation of $\sigma_{\phi\phi}$ vs. r for different values of t under Problem-I.

variable increases with the increase of time under each model.

Discussion on results of Problem-2:

Figures 5.1.2(a, b, c, d) reveal the distributions of the field variables under three models for the case of problem-2, i.e., when the boundary of the cavity is subjected to a unit step increase of temperature (thermal shock). Figure 5.1.2(a) displays that for this case, delay time has not much effect on displacement, u at any instant of time, t and all models predict almost similar results for displacement. However, we find from Figs. 5.1.2(b, c, d) that temperature and stress fields show prominent differences under different models and there is a significant role of the delay time parameter, τ. Figure

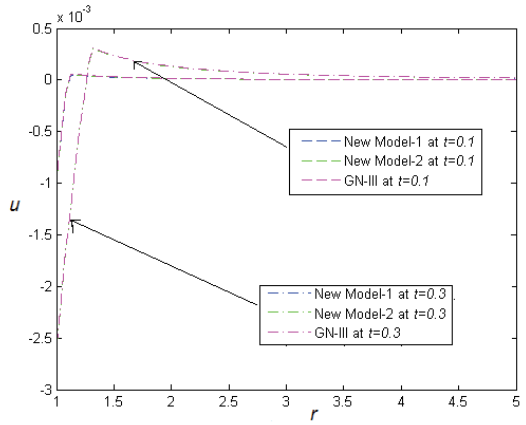

Fig. 5.1.2(a) : Variation of u vs. r for different values of t under Problem-2.

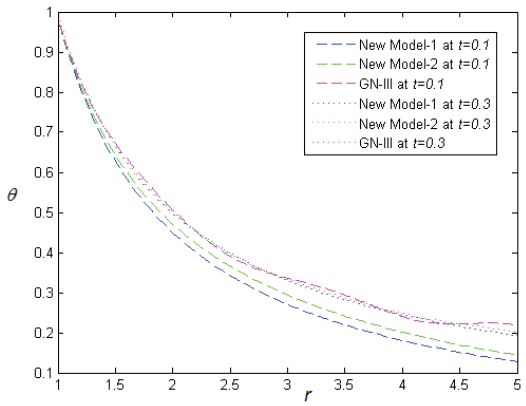

Fig. 5.1.2(b) : Variation of θ vs. r for different values of t under Problem-2.

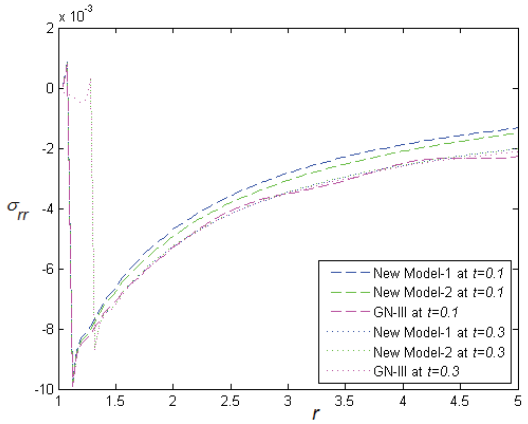

Fig. 5.1.2(c) : Variation of σ_{rr} vs. r for different values of t under Problem-2.

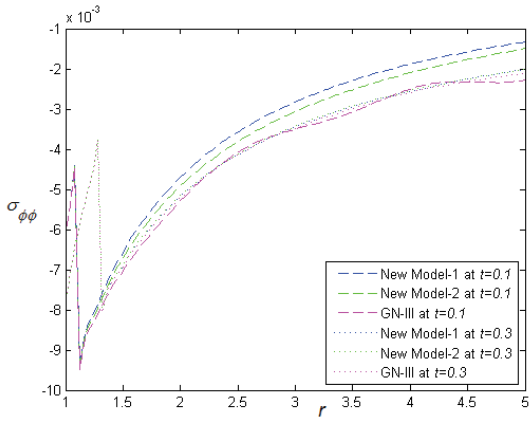

Fig. 5.1.2(d) : Variation of $\sigma_{\phi\phi}$ vs. r for different values of t under Problem-2.

5.1.2(b) shows that temperature θ increases with an increase in time t. Further, New model-I shows the highest value and GN-III predicts the lowest value for temperature θ at a fixed time t, i.e. τ has an increasing effect on temperature θ. Figures 5.1.2(c, d) indicate that as time increases, the stresses σ_{rr} and $\sigma_{\phi\phi}$ show oscillatory nature near the boundary of the cavity. However, σ_{rr} and $\sigma_{\phi\phi}$ decrease with an increase in time t as we move away from the boundary. σ_{rr} and $\sigma_{\phi\phi}$ show the highest value in the context of GN-III model and the lowest value for New model-I at a fixed time t i.e. there is a decreasing effect of τ on σ_{rr} and $\sigma_{\phi\phi}$. From Figs. 5.1.2(a, b, c, d), it is observed that effects of delay time parameter, τ, on the field variables for problem-2 is significant for temperature and stress variables. However, the effects decrease with an increase of time t, although the region of influence for each variable increases with time.

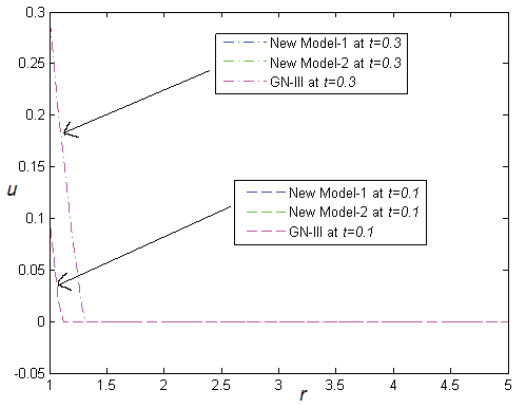

Fig. 5.1.3(a) : Variation of u vs. r for different values of t under Problem-3.

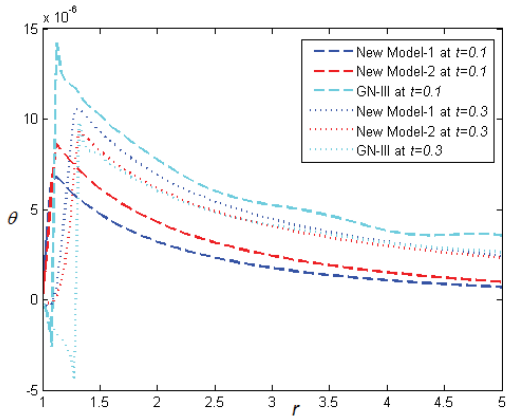

Fig. 5.1.3(b) : Variation of θ vs. r for different values of t under Problem-3.

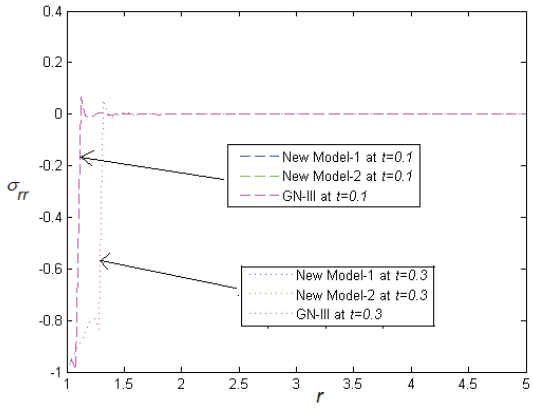

Fig. 5.1.3(c) : Variation of σ_{rr} vs. r for different values of t under Problem-3.

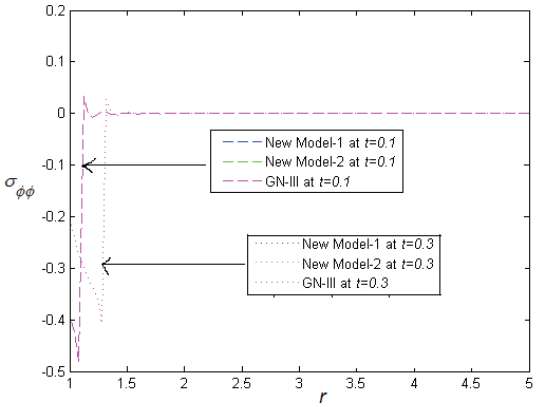

Fig. 5.1.3(d) : Variation of $\sigma_{\phi\phi}$ vs. r for different values of t under Problem-3.

Discussion on results of Problem-3:

Figures 5.1.3(a, b, c, d) reveal that for problem-3 when the boundary of the cavity is subjected to a normal load, there is no prominent effect of delay parameter on u, σ_{rr} and $\sigma_{\phi\phi}$. However, it affects the temperature, θ, very prominently. As in other cases, the region of influence for each field increases with respect to time t. Furthermore, Fig. 5.1.3(a) shows that at lower time, the GN-III model predicts the highest value and New model-I shows the lowest value for temperature θ. However, at higher time, the result is reverse i.e. GN-III model predicts the lowest value and New model-I predicts the highest value for θ.

5.1.10 Conclusion

In the present paper, we have investigated the thermoelastic interactions in an unbounded elastic medium with a spherical cavity under the very recent heat conduction model with single delay term introduced by Quintanilla (2011). This model is an alternative formulation of the three phase-lag model. We have studied the thermoelastic interactions in the isotropic elastic medium with a spherical cavity subjected to three types of thermal and mechanical loads named as problem-1, problem-2 and problem-3, in the contexts of two versions of this New model. We find analytical as well as numerical solutions for the distribution of the field variables displacement, temperature and stresses with the help of the integral transform technique. We also compare numerical results with the corresponding results of Green-Naghdi thermoelasticity theory of type-III. We observed following significant facts while analyzing the numerical and analytical results:

(1) In case of the problem-1, when the boundary of the cavity is subjected to a ramp type heating, we observe that elastic waves are propagating with finite speed. However, in the context of New model-I, it propagates without any attenuation although under New model-II, it decays exponentially with distance. In this problem, the speed of elastic waves do not depend on the delay parameter as well as any material parameters. On the other hand, thermal waves propagate with infinite speed like classical thermoelasticity theory. In this case, all the fields are continuous in nature and the results are of similar nature like GN-III model.

(2) In case of the problem-2, when the boundary of the cavity is subjected to thermal shock, we observe that elastic wave propagate with finite speed but attenuation coefficient of elastic wave for New model-II is totally dependent on the delay time and other material parameters. We also find that temperature and stress fields show prominent differences under different models and there is a significant role of the delay time parameter.

(3) In the case when the boundary of the cavity is subjected to a normal load, i.e. for problem-3, there is no prominent effect of delay parameter on u, σ_{rr} and $\sigma_{\phi\phi}$. However, it affects the temperature, θ, very prominently.

(4) In problem-2 and problem-3, we also observe that there is a finite discontinuity at elastic wavefront for radial and circumferential stress distribution under New model-I and New-model-II. Displacement and temperature are continuous in nature under these two problems. However, all fields are continuous in nature for problem-1.

5.2 An Investigation on Harmonic Plane Wave Propagation in a Thermoelastic Medium: a Detailed Analysis of a Recent Thermoelastic Model with Single Delay Term

---

5.2.1 Introduction

Propagation of harmonic plane waves in an elastic medium has been the center of active research for a long time. Plane waves can be defined as the waves whose wavefronts are infinitely long straight lines. Such waves travel in the direction perpendicular to the wavefronts. The propagation of harmonic plane waves in classical thermoelasticity was studied by Lessen (1957), Deresiewicz (1957), Chadwick and Sneddon (1958) and Chadwick (1960). Later on, Nayfeh and Nemat-Nasser (1971) and Puri (1973) had analyzed the propagation of plane waves in the context of Lord-Shulman theory, i.e., under the generalized thermoelasticity theory with one relaxation time. The propagation and stability of harmonically time-dependent thermoelastic plane waves in TRDTE was reported by Agarwal (1979). The wave propagation in Green-Lindsay model and Lord-Shulman model has been again studied by Haddow and Wegner (1996). Plane waves in the reference of thermoelasticity theory of GN-II is discussed by Chandrashekharaiah (1996). Prasad et. al. (2010) examined the propagation of plane waves under thermoelasticity with dual phase-lags. Puri and Jordan (2004) and Kothari and Mukhopadhyay (2012) explored the propagation of plane waves in GN-III thermoelasticity theory and highlighted several important features of this theory.

The content of this section is communicated to an international peer reviewed journal for publication

In this present section of the thesis, we have interpreted the propagation of plane harmonic waves in an isotropic unbounded medium in the context of the newly proposed thermoelastic model given by Quintanilla (2011). This model attempted to reformulate the heat conduction model that takes into account of the microstructural effects on heat transport phenomenon and provided an alternative heat conduction theory with a single delay term. We have studied the harmonic plane waves propagating in a thermoelastic medium by employing this new model and derived the exact dispersion relation solution of harmonic plane wave propagation. We also provide asymptotic expressions for several important characterizations of the wave fields, such as phase velocity, specific loss, penetration depth and amplitude ratio. The transverse mode wave is found to be uncoupled with the thermal field, whereas the longitudinal mode wave is coupled with the thermal field. Hence, we pay special attention to the longitudinal wave. We observe the presence of two different modes of the longitudinal wave and identify them as predominated elastic and thermal mode longitudinal wave. We further find the asymptotic expansions of several qualitative characterizations of the wave field such as phase velocity, specific loss and penetration depth for the high and low frequency values for this model. We also carry out computational work to obtain numerical results of the wave characterizations for the intermediate values of frequency and the results are illustrated graphically. The amplitude ratio of the thermal and the elastic wave is also investigated. We verify the analytical results predicting the limiting behavior of the wave characteristics with our numerical values of the above mentioned quantities. On the basis of analytical and numerical results, a thorough analysis of the effects of the single delay parameter on various wave characteristics is presented. We highlight several characteristic features of the new thermoelastic model as compared to the other model.

5.2.2 Basic Governing Equations

We consider an unbounded, isotropic and thermally conducting elastic medium. The constituent equations and basic governing equations for the thermoelastic interactions inside the medium in absence of body forces and heat sources in the contexts of the new thermoelastic model given by Quintanilla (2011) are considered as follows:

Stress-strain-temperature relation:

$$\sigma_{ij} = \lambda e \delta_{ij} + 2\mu e_{ij} - \beta(\theta - \theta_0)\delta_{ij} \tag{5.2.1}$$

Strain-displacement relation:

$$e_{ij} = \frac{1}{2}(u_{i,j} + u_{j,i}) \tag{5.2.2}$$

Equation of motion without body force:

$$\sigma_{ij,j} = \rho \ddot{u}_i \tag{5.2.3}$$

Displacement equation of motion without body force is obtained from Eqs. (5.2.1)–(5.2.3) as:

$$\mu u_{i,jj} + (\lambda + \mu) u_{j,ji} - \beta \theta_{,i} = \rho \ddot{u}_i \tag{5.2.4}$$

Heat conduction equation in the context of new model given by Quintanilla (2011) is taken in the form:

$$\left\{ k\frac{\partial}{\partial t} + k^*(1 + \tau\frac{\partial}{\partial t} + \frac{1}{2}\tau^2\xi\frac{\partial^2}{\partial t^2}) \right\} \nabla^2\theta = \beta\theta_0 \ddot{u}_{i,i} + \rho c_E \ddot{\theta} \tag{5.2.5}$$

Here τ is the delay parameter described by Quintanilla (2011) and ∇^2 is the Laplacian operator. The parameter ξ has been used here to formulate the problem under three

different models of heat conduction in a unified way. The case when we assume $\tau = 0$ in equation (5.2.5) corresponds to the heat conduction equation of thermoelasticity under GN-III model. In the case when $\tau \neq 0$, we obtain two different versions of heat conduction equation introduced by Quintanilla and Leseduarte (2013) by assuming $\xi = 1$ and $\xi = 0$. Here, in the second case (*i.e.*,when $\xi = 0$) the second order effect is neglected in the Taylor series approximation of the equation of heat conduction to the delay term.

Hence, we study our problem by considering equations (5.2.4) and (5.2.5), to analyze the results under three different cases as follows:

1. **New model – I** : $\tau \neq 0$, $\xi = 1$

2. **New model – II** : $\tau \neq 0$, $\xi = 0$

3. **GN III model** : $\xi = 0$, $\tau = 0$

To make the equations (5.2.4) and (5.2.4) simpler, we use the following transformations:

$u_i' = \frac{u_i}{c_0 t_o}$, $\theta' = \frac{\theta - \theta_0}{\theta_0}$, $x_i' = \frac{x_i}{c_o t_o}$, $t' = \frac{t}{t_o}$,$\tau' = \frac{\tau}{t_o}$, $c_0^2 = \frac{\lambda+2\mu}{\rho}$, $k_1 = \frac{k}{\rho c_E c_0^2 t_0}$, $k_2 = \frac{k^*}{\rho c_E c_0^2}$, $a_2 = \frac{\beta}{\rho c_E}$.

Here, $t_0(> 0)$, is the characteristic response in time for the medium.

Now, after dropping the primes for convenience, equations (5.2.4) and (5.2.5) change to the following forms:

$$\mu u_{i,jj} + (\lambda + \mu) u_{j,ji} - \beta \theta_0 \theta_{,i} = \rho c_0^2 \ddot{u}_i \tag{5.2.6}$$

$$\left\{ k_1 \frac{\partial}{\partial t} + k_2 (1 + \tau \frac{\partial}{\partial t} + \frac{1}{2} \tau^2 \xi \frac{\partial^2}{\partial t^2}) \right\} \nabla^2 \theta = a_2 \ddot{u}_{i,i} + \ddot{\theta} \tag{5.2.7}$$

We will study our problem in the contexts of three models simultaneously on the basis of the above two equations.

5.2.3 Dispersion Relation and its Derivation

The transverse waves remain uncoupled with the thermal field of the medium, whereas, in the case of longitudinal waves, the mechanical and thermal fields are coupled together. So, we are considering the solution of the longitudinal plane waves in the form

$$u_j = Ad_j e^{i(\omega t - \gamma n_i x_i)} \tag{5.2.8}$$

$$\theta = Be^{i(\omega t - \gamma x_i)} \tag{5.2.9}$$

where, ω is a positive real number called angular frequency of wave and γ is a complex constant. A and B are complex amplitudes (simultaneously not both zero). Here, d_j is the unit vector in the direction of displacement and n_j is the unit vector normal to wave front. $\frac{\omega}{\text{Real}(\gamma)}$, $\frac{\omega}{2\pi}$ and $\frac{2\pi}{\text{Real}(\gamma)}$ are phase velocity, frequency and wavelength of waves, respectively that correspond to the longitudinal waves. For our analysis, $\text{Real}(\gamma) > 0$ and $\text{Im}(\gamma) \leq 0$ must hold obviously for the wave to be physically realistic.

Now, substituting (5.2.8) and (5.2.9) into equations (5.2.6) and (5.2.7), we obtain

$$\begin{bmatrix} \omega^2 - \gamma^2 & -ia_1\gamma \\ ia_2\omega^2\gamma & (\gamma^2 k_2 - \frac{1}{2}\tau^2\xi\omega^2\gamma^2 k_2 - \omega^2) + i(\omega\tau k_2\gamma^2 + k_1\omega\gamma^2) \end{bmatrix} \begin{bmatrix} A \\ B \end{bmatrix} = \begin{bmatrix} 0 \\ 0 \end{bmatrix} \tag{5.2.10}$$

$a_1 = \frac{\beta\theta_0}{\lambda+2\mu}$.

Since for non-trivial solution of the system of equations (5.2.10), the determinant of the above system must be zero. Therefore, we obtain a bi-quadratic dispersion relation as

$$\gamma^4\left[k_2-\frac{1}{2}\tau^2\xi\omega^2k_2+i(k_1\omega+\tau k_2\omega)\right]$$
$$-\gamma^2\left[\omega^2+k_2\omega^2-\frac{1}{2}\tau^2\xi\omega^4k_2-a_1a_2\omega^2+i(k_1\omega^3+\tau k_2\omega^3)\right]+\omega^4=0 \tag{5.2.11}$$

Here, we observe from equation (5.2.11) that harmonic plane wave is clearly influenced by the delay term. Now by making coefficient of γ^4 real, we arrive at the simplified form of the dispersion relation

$$R(w)\gamma^4-(P-iQ)\gamma^2+(U-iV)=0 \tag{5.2.12}$$

where

$R(\omega)=r_1\omega^4+r_2\omega^2+r_3$, $P=p_1\omega^6+p_2\omega^4+p_3\omega^2$, $Q=q_1\omega^3$, $U=-u_1\omega^6+u_2\omega^4$, $V=v_1\omega^5$,

and

$r_1=p_1=\frac{1}{4}\xi^2\tau^4k_2^2,\ r_2=k_1^2+2k_1k_2\tau-\xi\tau^2k_2^2,\ r_3=k_2^2,$

$p_2=k_1^2+2k_1k_2\tau-\frac{1}{2}\xi\tau^2k_2h+\tau^2k_2^2-\xi\tau^2k_2^2,\ \ p_3=k_2^2+k_2h,$

$q_1=k_1h+\tau k_2h,$, $u_1=\frac{1}{2}\xi\tau^2k_2,\ u_2=k_2,\ \ v_1=(k_1+\tau k_2),\ h=1+\epsilon,\ \epsilon=a_1a_2.$

The equation (5.2.12) is therefore the unified form of the dispersion relation for the New model-I, New model-II and GN-III models and it clearly shows the effect of single delay term τ on the longitudinal plane waves. We observe that the dispersion relation (5.2.12) for the case when $\xi=0,\tau=0$, i.e., for GN-III model match perfectly with the corresponding relation derived by Puri and Jordan (2004).

5.2.4 Solution of Dispersion Relation

If roots of the equation (5.2.12) are $\pm\gamma_1$ and $\pm\gamma_2$, then we can write

$$\gamma_{1,2}^2 = \frac{(P - iQ) \pm \sqrt{D(\omega)}}{2R(\omega)} \tag{5.2.13}$$

where

$\text{Real}(D(\omega)) = p_1^2\omega^{12} + M_1\omega^{10} + M_2\omega^8 + M_3\omega^6 + M_4\omega^4$,

$\text{Im}(D(\omega)) = N_1\omega^9 + N_2\omega^7 + N_3\omega^5$,

$M_1 = (2p_1p_2 - 4r_1u_1)$, $M_2 = (p_2^2 + 2p_1p_3 - 4r_2u_1 - 4r_1u_2)$,

$M_3 = (2p_2p_3 - q_1^2 - 4r_3u_1 - 4r_2u_2)$, $M_4 = (p_3^2 - 4r_3u_2)$,

$N_1 = -2p_1q_1 + 4r_1v_1$, $N_2 = -2p_2q_1 + 4r_2v_1$, $N_3 = (-2p_3q_1 + 4r_3v_1)$.

Here, it is to be mentioned that among the four roots of γ, only two have negative imaginary parts. We will consider only those two roots with negative value of decay coefficient, $\text{Im}(\gamma)$. Now, equation (5.2.13) can be solved by applying the following theorem of complex numbers:

Theorem (Ponnusamy (2005) : For a given $z = x + iy \in \mathbb{C}$, the solutions of $w^2 = z$ are given by

$$w = \left[\sqrt{\frac{|z| + x}{2}} + i\,\text{sgn}(y)\sqrt{\frac{|z| - x}{2}}\right], \text{ where, } \text{sgn}(y) = \begin{cases} +1 & \text{if } y \geq 0 \\ -1 & \text{if } y < 0 \end{cases}$$

Using above theorem in (5.2.13), we can find two values of γ, whose imaginary parts are negative. These two values of γ correspond to two types of the longitudinal (dilatation) waves in which the first one is denoted as predominantly elastic wave and second one is thermal wave in nature. We denote γ related with first one by γ_1 and second one by γ_2.

5.2.5 Analytical Results

Since the general analysis of waves on the basis of the roots given by (5.2.13) is highly complicated, we therefore concentrate on the analysis of wave and effects of delay term under two special cases which correspond to the waves of very high and very low frequency.

Hence, we first obtain the asymptotic expressions for γ_1 and γ_2 from equation (5.2.13) by using the above theorem under these two special cases by assuming ω to be very large and very small, respectively. The results for the case of GN-III model are reported by Puri and Jordan (2004). Therefore, we skip to derive the analytical results of GN-III model and for the other two models, we proceed as follows:

5.2.5.1 Case-I: High Frequency Asymptotic Expansions

In this case, we assume that ω to be very large, i.e., $\omega \gg 1$. Hence, expanding (5.2.13) for large ω and neglecting higher powers of $\frac{1}{\omega}$, we write (5.2.13) as

$$\gamma_{1,2}^2 = \frac{-(P - iQ) \pm (S + iT)}{2R(\omega)}$$

where,

$$S = p_1\omega^6 + \frac{M_1}{2p_1}\omega^4 + \left(\frac{-M_1^2 + 4M_2p_1^2}{8p_1^3}\right)\omega^2 + \left(\frac{M_1^3 - 4M_1M_2p_1^2 + 2N_1^2p_1^2 + 8M_3p_1^4}{8p_1^3}\right) + O(\frac{1}{\omega^2})$$

and

$$T = \frac{N_1}{2p_1}\omega^3 + \frac{M_1N_1 - 2N_2p_1^2}{4p_1^3}\omega + \left(\frac{3M_1^2N_1 - 4M_2N1p_1^2 - 4M_1N_2p_1^2 + 8N_3p_1^4}{16N_1p_1^5}\right)\frac{1}{\omega} + O(\frac{1}{\omega^3})$$

Analytical results for $\gamma_{1,2}$:

For large values of ω, expanding above equation for $\gamma_{1,2}^2$ and neglecting higher powers of $\frac{1}{\omega}$, again by using the theorem of complex analysis as mentioned above, we finally obtain the asymptotic expansion of the roots of equation (5.2.13) for New model-I and New model-II as follows:

$\gamma_{1,2}$ for New model- I:

$$\gamma_1 \approx \sqrt{\frac{p_1}{r_1}}\omega\left(1+\frac{r_1A_1}{2p_1}\frac{1}{\omega^2}+\frac{r_1(4A_2p_1-r_1A_1^2)}{8p_1^2}\frac{1}{\omega^4}\right)$$
$$+i\frac{B_1\sqrt{r_1}}{2\sqrt{p_1}}\frac{1}{\omega^2}\left(1-\frac{(r_1A_1B_1-2B_2p_1)}{2B_1p_1}\frac{1}{\omega^2}\right)\text{as}\,(\omega\to\infty) \tag{5.2.14}$$

$$\gamma_2 \approx \frac{D_1}{2\sqrt{C_1}}\frac{1}{\omega}\left(1+\frac{8C_1^2D_1D_2-4C_1C_2D_1^2-D_1^4}{8C_1^2D_1^2}\frac{1}{\omega^2}\right)$$
$$+i\sqrt{C_1}\left(1+\frac{4C_1C_2+D_1^2}{8C_1^2}\frac{1}{\omega^2}\right)\text{as}\,(\omega\to\infty) \tag{5.2.15}$$

where

$A_1=\frac{1}{2r_1^2}\left((\frac{M_1}{2p_1}+p_2)-2p_1r_2\right)$

$A_2=\frac{1}{2r_1^3}\left((\frac{-M_1^2-4M_2p_1^2}{8p_1^3}+p_3)r_1^2-(\frac{M_1}{2p_1}+p_2)r_1r_2-2p_1(r_2^2-r_1r_2)\right)$

$B_1=\frac{1}{2p_1r_1}(N_1-2p_1q_1)$, $B_2=\frac{1}{2r_1^2}\left((\frac{-M_1N_1+2N_2p_1^2}{N_1p_1^3})+2r_2(-\frac{N_1}{p_1}+2q_1)\right)$

$C_1=\frac{1}{2r_1}(\frac{M_1}{2p_1}-p_2)$, $C_2=\frac{1}{2r_1^2}\left((\frac{M_1^2-4M_2p_1^2}{8p_1^3}+p_3)r_1-r_2(-\frac{M_1}{2p_1}+p_2)\right)$

$D_1=\frac{1}{2p_1r_1}(-N_1+2p_1q_1)$, $D_2=\frac{1}{8r_1^2}((-M_1N_1+2N_2p_1^2)r_1+2(N_1+2p_1q_1)r_2)$

$\gamma_{1,2}$ for New model- II:

$$\gamma_1 \approx \omega\left(1+\frac{(4A_1^{'}+B_1^{'2})}{`8}\frac{1}{\omega^2}\right)$$
$$+i\frac{B_1^{'}}{2}\left(1-\frac{B_1^{'}(4A_1^{'}+B_1^{'2})-8B_2^{'})}{8B_1^{'}}\frac{1}{\omega^2}\right)\text{as}\,(\omega\to\infty) \tag{5.2.16}$$

$$\gamma_2 \approx \sqrt{\frac{D_1^{'}}{2}}\sqrt{\omega}\left(1+\frac{C_1^{'}}{2D_1^{'}}\frac{1}{\omega}+\frac{4D_1^{'}D_2^{'}+C_1^{'2}}{8D_1^{'2}}\frac{1}{\omega^2}\right)$$
$$+i\sqrt{\frac{D_1^{'}}{2}}\sqrt{\omega}\left(1-\frac{C_1^{'}}{2D_1^{'}}\frac{1}{\omega}+\frac{4D_1^{'}D_2^{'}+C_1^{'2}}{8D_1^{'2}}\frac{1}{\omega^2}\right)\text{ as }(\omega\to\infty) \tag{5.2.17}$$

where

$A_1^{'}=\frac{1}{2r_1^2}\left((\frac{N_2^2+4M_3p_2^2}{8p_3^2}+p_3)r_2-2p_2r_3\right)$, $B_1^{'}=\frac{1}{4r_2}(\frac{N_2}{p_2}-2q_1)$,

$B_2^{'}=\frac{1}{32r_2^2}\left(\frac{N_2^3+4M_3N_2p_2^2-8N_3p_2^4}{p_2^5}-8(\frac{N_2}{p_2}-2q_1)r_3\right)$, $C_1^{'}=\frac{1}{2r_2}\left(p_3-\frac{N_2^2}{8p_2^3}\right)$,

$D_1^{'}=\frac{1}{4r_2}\left(2q_1+\frac{N_2}{p_2}\right)$, $D_2^{'}=\frac{(N_2^3+4M_3N_2p_2^2-8N_3p_2^4)r_2+8(\frac{N_2}{p_2}+2q_1)r_3}{32r_2^3\omega^2}$.

5.2.5.2 Case- II: Low Frequency Asymptotic Expansions

We use the similar approach as above for the low frequency asymptotic expressions of different wave fields, and find the required roots of equation (5.2.13) by considering ω to be very very small, i.e., by assuming $\omega \ll 1$. Interestingly, we get the exactly similar results for New model- I and New model-II and they are obtained as follows:

$\gamma_{1,2}$ for New model- I/New model-II

$$\gamma_1 \approx \sqrt{E_1}\omega\left(1+\frac{4E_1E_2+F_1^2}{8E_1^2}\omega^2\right)-i\frac{F_1}{2\sqrt{E_1}}\omega^2(1+\frac{8E_1^2F_2-4E_1E_2F_1-F_1^3}{8F_1E_1^2}\omega^2)(\omega\to 0) \tag{5.2.18}$$

$$\gamma_2 \approx \sqrt{G_1}\omega\left(1+\frac{4G_1G_2+H_1^2}{8G_1^2}\omega^2\right)-i\frac{H_1}{2\sqrt{G_1}}\omega^2(1+\frac{8G_1^2H_2-4G_1G_2H_1-H_1^3}{8H_1G_1^2}\omega^2)(\omega\to 0) \tag{5.2.19}$$

where,

$E_1=\frac{\sqrt{M_4}+p_3}{2r_3}$, $E_2=\frac{1}{2r_3^2}\left[-(\sqrt{M_4}+p_3)r_2+(\frac{4M_3M_4+N_3^2}{8M_4^{3/2}}+p_2)r_3\right]$

$$F_1 = \frac{1}{4r_3}(\frac{N_3}{\sqrt{M_4}} - 2q_1), F_2 = \frac{1}{32r_3^2}\left[-8((\frac{N_3}{\sqrt{M_4}} - 2q_1)r_2 + \frac{(-8M_4^2N_2+4M_3M_4N_3+N_3^3)r_3}{M_4^{5/2}})\right]$$

$$G_1 = \frac{-\sqrt{M_4}+p_3}{2r_3}, G_2 = \left[(\sqrt{M_4} - p_3)r_2 + (-\frac{4M_3M_4+N_3^2}{8M_4^{3/2}} + p_2)r_3\right]$$

$$H_1 = -\frac{1}{4r_3}(\frac{N_3}{\sqrt{M_4}} + 2q_1), H_2 = \frac{1}{32r_3^2}\left[8((\frac{N_3}{\sqrt{M_4}} + 2q_1)r_2 - \frac{(-8M_4^2N_2+4M_3M_4N_3+N_3^3)r_3}{M_4^{5/2}})\right]$$

5.2.6 Asymptotic Results for Different Wave Fields

Now, we make an attempt to derive the asymptotic expressions of the important wave components, like phase velocity, specific loss, penetration depth and amplitude ratio of both the modified elastic waves and thermal mode longitudinal waves and study the wave characteristics under the case of high frequency values as well as low frequency values. Here, we see that in case of low frequency asymptotic expansion of all wave components, we get the similar expression for the New model -I and New model- II.

5.2.6.1 Phase Velocity

The phase velocity of wave is given by the formula

$$V_{E,T} = V_{1,2} = \frac{\omega}{\text{Real}(\gamma_{1,2})} \tag{5.2.20}$$

where, V_E and V_T represent the phase-velocities of elastic mode and thermal mode waves, respectively.

With the help of equations (5.2.14) - (5.2.19), and using the formula (5.2.20), we find the high frequency and low frequency asymptotic expressions for V_E and V_T as follows:

High frequency asymptotes of phase velocities

New model- I:

$$V_E \sim \left\{1 - \frac{A_1}{2}\frac{1}{\omega^2} + o\left(\frac{1}{\omega^4}\right)\right\} \tag{5.2.21}$$

$$V_T \sim \frac{2\sqrt{C_1}}{D_1}\omega^2\left[1 - \frac{8C_1^2D_2 - 4C_1C_2D_1 - D_1^3}{8C_1^2D_1^3}\frac{1}{\omega^2} + o\left(\frac{1}{\omega^4}\right)\right] \tag{5.2.22}$$

New model -II:

$$V_E \sim \left\{1 - \frac{(4A_1^{'} + B_1^{'2})}{16}\frac{1}{\omega^2} + o\left(\frac{1}{\omega^4}\right)\right\} \tag{5.2.23}$$

$$V_T \sim \sqrt{\frac{2}{D_1^{'}}}\sqrt{\omega}\left[1 - \frac{C_1^{'}}{2D_1^{'}}\frac{1}{\omega} + \frac{-4D_1^{'}D_2^{'} + C_1^2}{8D_1^{'2}}\frac{1}{\omega^2}\right] \tag{5.2.24}$$

Low frequency asymptotes of phase velocities

for New model -I/New model- II:

$$V_E \backsim \frac{1}{\sqrt{E_1}}\left[1 - \frac{1}{8E_1^2}(4E_1E_2 + F_1^2)\omega^2 + o\left(\omega^4\right)\right] \tag{5.2.25}$$

$$V_T \backsim \frac{1}{\sqrt{G_1}}\left[1 - \frac{1}{8G_1^2}(4G_1G_2 + F_1^2)\omega^2 + o\left(\omega^4\right)\right] \tag{5.2.26}$$

5.2.6.2 Specific Loss

We define specific loss as the ratio of energy dissipated per stress cycle to the total vibration energy, which is given as

$$\left(\frac{\triangle W}{W}\right)_{E,T} = \left(\frac{\triangle W}{W}\right)_{1,2} = 4\pi\frac{|\ \mathrm{Im}(\gamma_{1,2})\ |}{|\ \mathrm{Real}(\gamma_{1,2})\ |} \tag{5.2.27}$$

where, $\left(\frac{\triangle W}{W}\right)_E$ and $\left(\frac{\triangle W}{W}\right)_T$ are the specific losses of elastic and thermal waves, respectively.

With the help of equations (5.2.14) - (5.2.19), and using this formula (5.2.27), we find the high frequency and low frequency asymptotic expressions for $\left(\frac{\triangle W}{W}\right)_E$ and $\left(\frac{\triangle W}{W}\right)_T$ as follows:

High frequency asymptotic expansions of specific loss

New model -I:

$$\left(\frac{\triangle W}{W}\right)_E \sim 2\pi B_1 \frac{1}{\omega^3}\left\{1+\frac{B_2}{B_1}\frac{1}{\omega^2}+o(\frac{1}{\omega^4})\right\} \tag{5.2.28}$$

$$\left(\frac{\triangle W}{W}\right)_T \sim \frac{8\pi C_1}{D_1}\omega\left\{(1+\frac{D_2}{D_1}\frac{1}{\omega^2}+o(\frac{1}{\omega^4})\right\} \quad \text{as } \omega\to\infty \tag{5.2.29}$$

New model- II:

$$\left(\frac{\triangle W}{W}\right)_E \sim 2\pi B_1^{'}\frac{1}{\omega}\left\{1-\frac{8A_1^{'}B_1^{'}+2B_1^{'3}-8B_1^{'}}{8B_1^{'}}\frac{1}{\omega^2}+o(\frac{1}{\omega^4})\right\} \tag{5.2.30}$$

$$\left(\frac{\triangle W}{W}\right)_T \sim 4\pi\left\{(1-\frac{C_1^{'}}{D_1^{'}}\frac{1}{\omega}+\frac{C_1^{'2}}{2D_1^{'2}}\frac{1}{\omega^2}\right\} \quad \text{as } \omega\to\infty \tag{5.2.31}$$

Low frequency asymptotic expansions of specific loss

for New model- I/New model -II:

$$\left(\frac{\triangle W}{W}\right)_E \sim \frac{2\pi F_1}{E_1}\omega\left[1+\frac{4E_1^2F_2-4E_1E_2F_1-F_1^3}{E_1^2F_1}\omega^2+o(\omega^4)\right] \tag{5.2.32}$$

$$\left(\frac{\triangle W}{W}\right)_T \sim \frac{2\pi G_1}{H_1}\omega\left[1+\frac{4G_1^2H_2-4G_1G_2H_1-F_1^3}{G_1^2H_1}\omega^2+o(\omega^4)\right] \quad \text{as } \omega\to 0 \tag{5.2.33}$$

5.2.6.3 Penetration Depth

We define penetration depth by the following relation:

$$\delta_{E,T} = \delta_{1,2} = \frac{1}{|\ \mathrm{Im}(\gamma_{1,2})|} \tag{5.2.34}$$

where, δ_E and δ_T are the penetration depths of elastic and thermal waves, respectively. With the help of equations (5.2.14) - (5.2.19), and (5.2.34) we find the high frequency and low frequency asymptotic expressions for δ_E and δ_T from the above formula as follows:

High frequency asymptotic expansions of penetration depth

New model- I:

$$\delta_E \sim \frac{2}{B_1}\omega^2 \left(1 + \frac{(A_1B_1 - 2B_2)}{2B_1}\frac{1}{\omega^2} + o(\frac{1}{\omega^4})\right) \tag{5.2.35}$$

$$\delta_T \sim \frac{1}{\sqrt{C_1}} \left(1 - \frac{4C_1C_2 + D_1^2}{8C_1^2}\frac{1}{\omega^2} + o(\frac{1}{\omega^4})\right) \quad as\ \omega \to \infty \tag{5.2.36}$$

New model- II:

$$\delta_E \sim \frac{2}{B_1'} \left(1 + \frac{B_1'(4A_1' + B_1'^2) - 8B_2')}{8B_1'}\frac{1}{\omega^2}\right) \tag{5.2.37}$$

$$\delta_T \sim \sqrt{\frac{2}{D_1'}}\frac{1}{\sqrt{\omega}} \left(1 + \frac{C_1'}{2D_1'}\frac{1}{\omega} + \frac{-4D_1'D_2' + C_1^2}{8D_1'^2}\frac{1}{\omega^2}\right) \quad as\ \omega \to \infty \tag{5.2.38}$$

Low frequency asymptotic expansions penetration depth

for New model -I/New model -II:

$$\delta_E \sim \frac{2\sqrt{E_1}}{F_1}\frac{1}{\omega^2}(1 - \frac{8E_1^2F_2 - 4E_1E_2F_1 - F_1^3}{8F_1E_1^2}\omega^2) \tag{5.2.39}$$

$$\delta_T \sim \frac{2\sqrt{G_1}}{H_1}\frac{1}{\omega^2}(1 - \frac{8G_1^2H_2 - 4G_1G_2H_1 - H_1^3}{8H_1G_1^2}\omega^2) \quad (\omega \to 0) \tag{5.2.40}$$

5.2.6.4 Amplitude Ratio

In view of equations. (5.2.8), (5.2.9) and (5.2.10), we find that the amplitude ratios of elastic and thermal mode longitudinal wave as

$$\psi_{E,T} = |\frac{B}{A}| = \frac{1}{a_1}|\gamma_{E,T} - \frac{\omega^2}{\gamma_{E,T}}| \tag{5.2.41}$$

Here, ψ_E and ψ_T are the amplitude ratio of elastic and thermal waves, respectively.

Now, with the help of equations (5.2.14) - (5.2.19), and (5.2.41) we find the high frequency and low frequency asymptotic expressions for ψ_E and ψ_T from the above formula as follows:

High frequency asymptotes of amplitude ratios

for New model- I:

$$\psi_E = \frac{A_1}{a_1\omega}\left(1 + \frac{(B_1^2 - \frac{3A_1^3}{4})}{2A_1^2}\frac{1}{\omega^2} + o(\frac{1}{\omega^4})\right) \tag{5.2.42}$$

$$\psi_T = \frac{\omega^2}{a_1\sqrt{C_1}}\left(1 - \frac{(4C_1^3 + 2C_1C_2 + D_1^2)}{4C_1^2}\frac{1}{\omega^2} + o(\frac{1}{\omega^4})\right) \tag{5.2.43}$$

New model- II:

$$\psi_E = \frac{B_1^{'}}{a_1}\left(1 + \frac{1}{16B_1^2}(16A_1^{'2} - A_1^{'}B_1^{'2} + 32B_1^{'}B_2^{'} - 4B_1^{'4})\right)\frac{1}{\omega^2} + o(\frac{1}{\omega^4}) \tag{5.2.44}$$

$$\psi_T = \frac{\omega^{\frac{3}{2}}}{a_1\sqrt{D_1^{'}}}\left(1 - \frac{D_1^{'}}{\omega} + \frac{C_1^{'2}}{8D_1^{'2}}\frac{1}{\omega^2}\right) \tag{5.2.45}$$

Low frequency asymptotes of amplitude ratios:

for New model- I/New model -II:

$$\psi_E = \frac{(E_1 - 1)\omega}{a_1\sqrt{E_1}}\left(1 + \frac{(4E_1^2E_2 + 4E_1E_2 + F_1^2 - F_1^2E_1)}{4E_1^2(E_1 - 1)}\omega^2 + o(\omega^4)\right) \tag{5.2.46}$$

$$\psi_T = \frac{(G_1-1)\omega}{a_1\sqrt{G_1}}\left(1+\frac{(4G_1^2G_2+4G_1G_2+H_1^2-H_1^2G_1)}{4G_1^2(G_1-1)}\omega^2+o(\omega^4)\right) \tag{5.2.47}$$

5.2.7 Numerical Results

In order to interpret the asymptotic results obtained in the previous section and to look into the nature of various wave components in details, we have made an attempt to find the numerical values of different wave characterizations for both the thermal and elastic mode longitudinal waves for intermediate values of frequency. For this, we have assumed $\epsilon = 0.0168$, $h = 1.0168$, $\tau = 0.01, k_1 = 1$. Using the Mathematica software, we have generated codes to compute the numerical values of different components directly from equation (5.2.13) and by using the formulas expressed by equations (5.2.20), (5.2.27), (5.2.34) and (5.2.41). The computation for the values of phase velocity, specific loss, penetration depth under all three cases (New model- I, New model- II and GN- III) for different values of frequency, ω are carried out and the results are presented in different figures. In all the figures, we observe the variation of different wave characteristics with frequency in the contexts of these three models. Both low and high frequency cases are shown separately in order to show the limiting behaviour of the wave fields. We also show the variations of the wave fields with thermal conductivity rate, k^*.

5.2.8 Analysis of Analytical and Numerical Results

Phase velocity:

Figure 5.2.1(a) represents the variation of elastic phase velocity for low frequency case. It shows that the phase velocity V_E of elastic mode wave, under New model-I, New model-II and GN-III model are almost same for a fixed value of k_2. However, there is prominent difference for different k_2 under each model. V_E approaches to a constant value as $\omega \to 0$

under each model and for each value of k_2. This limiting value (equal to $\frac{1}{\sqrt{E_1}}$ as clear from the analytical result, given by equation (5.2.25)) is same for each model but it is dependent on k_2. At $k_2 = k_1 = 1$, its value is 0.9372. For $k_2 < k_1$, there are two corner points in the plots of V_E indicating the existence of two critical frequencies corresponding to these points. The location of the corner point shifts right as k_2 increases. For $k_1 \geq k_2$, there exist a local maxima for V_E under each model, while in case of $k_2 > k_1$, V_E is non-decreasing and reaches to a constant limiting value which is the maximum for it.

Plots of elastic mode phase velocity, V_E for high frequency under the different models is depicted in the Fig. 5.2.1(b). It is observed that as $\omega \to \infty$, V_E approaches to a constant value equal to 1 under all models and for each value of k_2. This fact is also very clear from the analytical results shown by the equations (5.2.21) and (5.2.23). Our analytical results show that the limiting constant value is same for each model and is free from k_2. We also observe from numerical results that there is no prominent difference in V_E under different models with a fixed value of k_2 for high frequency too.

Figure 5.2.2(a,b) show the variation of phase velocity V_T of thermal model longitudinal wave for low and high values of ω. Figure 5.2.2(a) shows that there is no prominent difference in V_T nearer to $\omega = 0$, for a fixed k_2 in the different models. While as ω increases, the difference in V_T is prominent for different models. The plots for different k_2 show significant difference. We note that V_T approaches to a constant (equal to $\frac{1}{\sqrt{G_1}}$ as shown in analytical result given by equation (5.2.26) value as $\omega \to 0$. This constant is same for all models for a fixed k_2 but it is different for the different value of k_2 (as G_1 dependent on k_2). As in case of V_E, there is also corner points in the graph of V_T for $k_2 < k_1 = 1.00$ and the point shifts right as k_2 increases. Figure 5.2.2(b) shows that $V_T \to \infty$ as $\omega \to \infty$ under all three models which is in agreement with the analytical result given by the equations (5.2.22) and (5.2.24). For the range of frequency (ω), between 10-200, the effect of k_2 disappears for V_T but beyond this range, again there is a significant effect of k_2 on V_T. Furthermore, it is observed that as ω increases, the difference in V_T predicted by different

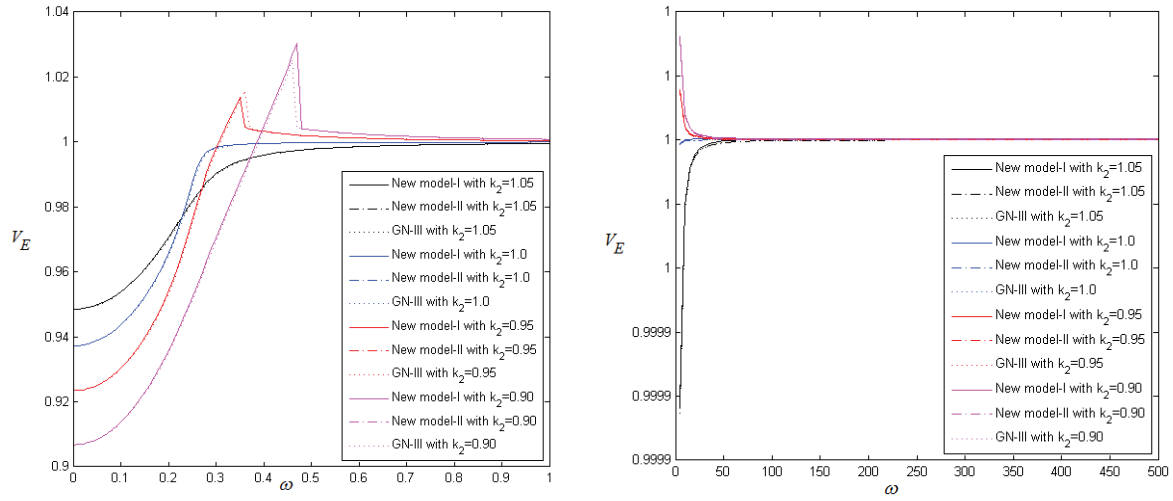

(a) (b)

Figs. 5.2.1(a,b): Variation of phase velocity of elastic wave (V_E) with low and high frequency (ω) respectively

models increases as well.

Specific Loss :

The variation of specific loss, $\left(\frac{\triangle W}{W}\right)_E$ of elastic wave for low and high frequency is shown in the Figs. 5.2.3(a,b), respectively. The Fig. 5.2.3(a) shows that there is not much difference in $\left(\frac{\triangle W}{W}\right)_E$ for lower values of ω under the different models while each model predicts differently for specific loss of elastic mode wave for different values of k_2. The specific loss $\left(\frac{\triangle W}{W}\right)_E \to 0$ as $\omega \to 0$ under each model and for every value of k_2(this is also clear from the analytical result given by equation (5.2.32)). Like the phase velocity, for $k_2 < k_1$, there are critical frequencies for $\left(\frac{\triangle W}{W}\right)_E$ under all the models and they show corner points in the plots of specific loss of elastic wave. Figure 5.2.3(b) shows that as frequency increases, all models shows similar nature with respect to k_2. Also $\left(\frac{\triangle W}{W}\right)_E \to 0$ as $\omega \to \infty$ for all values of k_2 and under each model which is in agreement with the analytical result given by equations (5.2.28) and (5.2.30).

Figures 5.2.4(a,b) shows the variation for specific loss, $\left(\frac{\triangle W}{W}\right)_T$ of thermal mode wave for low and high values of ω. Figure 5.2.4(a) shows that only nearer to $\omega = 0$, different models

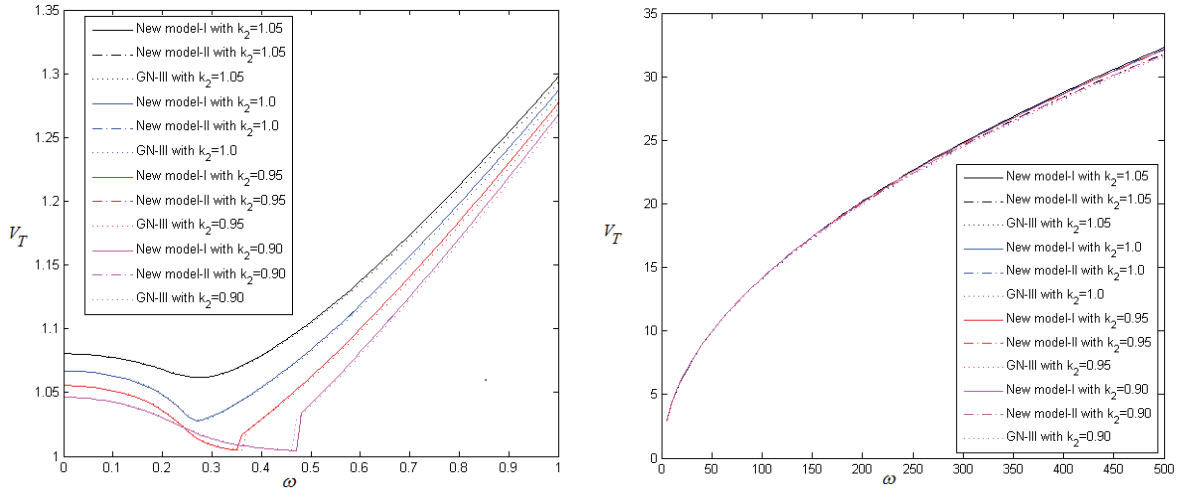

(a) (b)

Figs. 5.2.2(a,b): Variation of phase velocity of thermal wave (V_E) with low and high frequency (ω) respectively

predict similarly for specific loss of thermal wave for fixed k_2 but as ω starts increasing, the difference in predictions by different models becomes prominent. As usual the critical frequency also exist for $\left(\frac{\triangle W}{W}\right)_T$ corresponding to each models for $k_2 \leq k_1$. It is shown by Fig. 5.2.4(b) that for higher values of ω, the difference in $\left(\frac{\triangle W}{W}\right)_T$ is prominent for different k_2 under all models. The Fig. 5.2.4(b) also shows one vary significant observation that as $\omega \to \infty$, $\left(\frac{\triangle W}{W}\right)_T$ approaches to ∞ for New model-I, whereas $\left(\frac{\triangle W}{W}\right)_T$ approaches to constant value under New model-II and GN-III model. This fact is in complete agreement with our analytical result as given by equation (5.2.31).

Penetration Depth:

Figures 5.2.5(a,b) shows the variation for phase velocity δ_E of an elastic wave for low and high values of ω. Figure. 5.2.5(a) shows that there is no difference in δ_E under different thermoelastic theories for a fixed k_2, while some differences in δ_E for a particular model is observed with respect to the variation in k_2. Further, $\delta_E \to \infty$ as $\omega \to 0$ for each model and for each value of k_2 which is clear from the analytical result given by equation (5.2.37). The Fig. 5.2.5(b) shows that for very high frequency values, there is a prominent difference

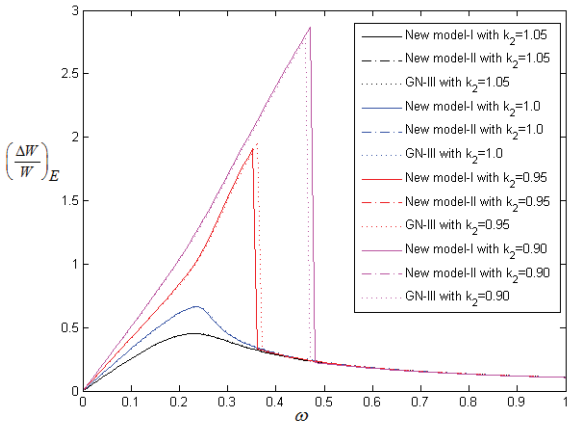

(a)

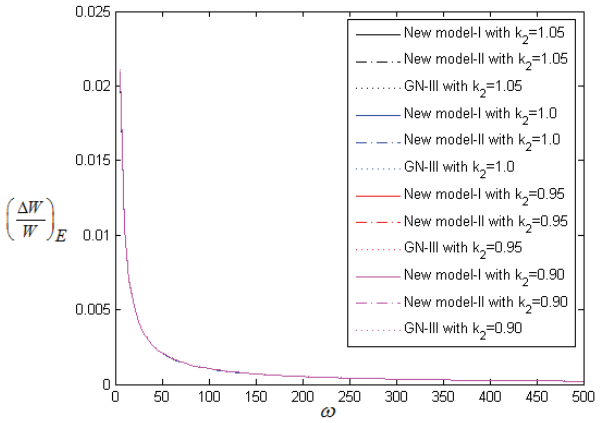

(b)

Figs. 5.2.3(a,b): Variation of specific loss of elastic wave $\left(\frac{\triangle W}{W}\right)_E$ with low and high frequency (ω) respectively

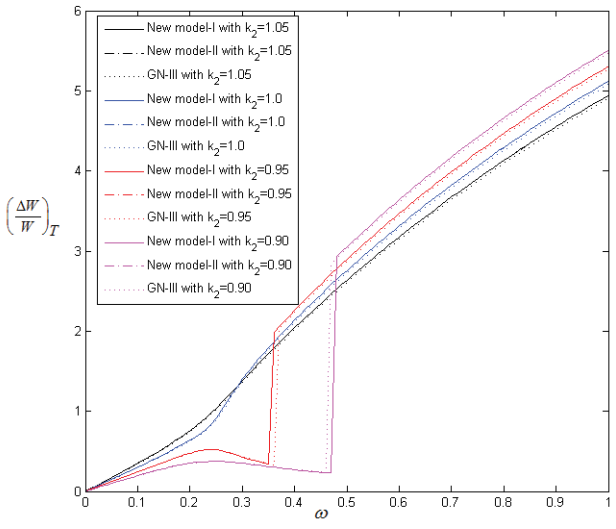

(a)

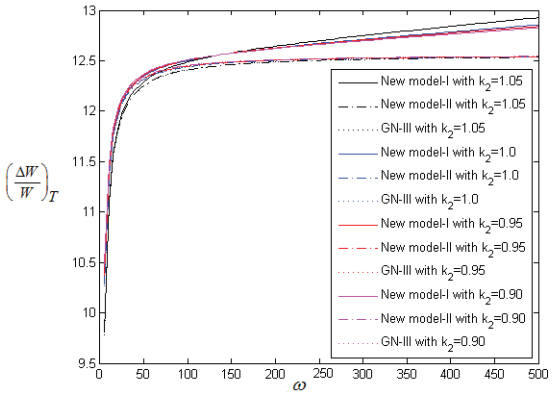

(b)

Figs. 5.2.4(a,b): Variation of specific loss of elastic wave $\left(\frac{\triangle W}{W}\right)_T$ with low and high frequency (ω) respectively

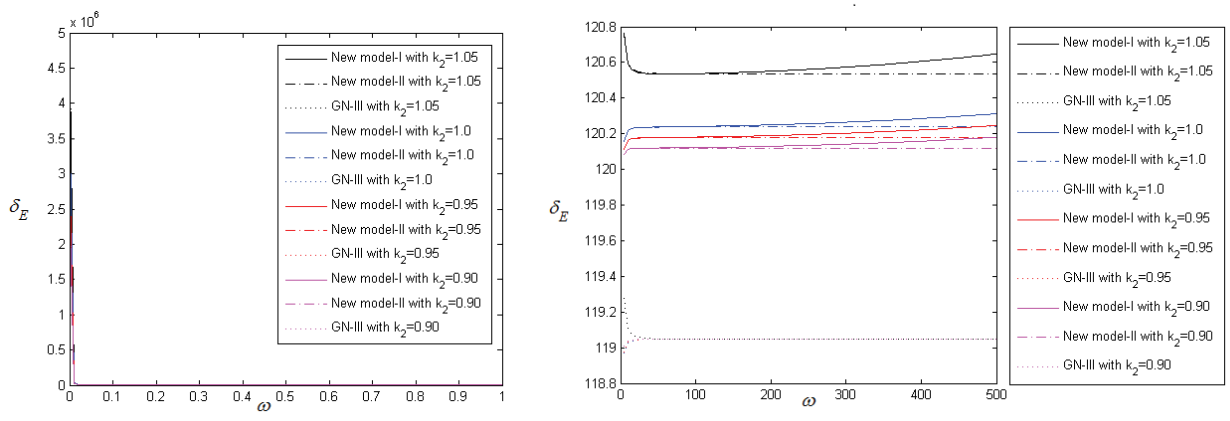

(a) (b)

Figs. 5.2.5(a,b): Variation of penetration depth of elastic wave δ_E with low and high frequency (ω) respectively

in δ_E for different models and with respect to k_2 as well. Further, from our analytical result (see equation (5.2.37)) as well as from numerical result (Fig. 5.2.5(b)), we get clear indication that for a fixed k_2, $\delta_E \to \infty$ as $\omega \to \infty$ under New model-I. However, in the contexts of New model-II and GN-III model, $\delta_E \to$ constant value (as $\delta_E \to \frac{2}{B_1}$ for New model-2 is clear from equation (5.2.37) which is equal to 120.226 for $k_2 = 1$) as $\omega \to \infty$.

Figures 5.2.6(a,b) shows the variation of the penetration depth of thermal wave under the different thermoelasticity theories for low and high frequency, respectively. Figures 5.2.6(a,b) show that there is no prominent difference in δ_T for low as well as for high frequency values with respect to different models and different k_2. Further, Fig. 5.2.6(a) shows that like the case of δ_E, $\delta_T \to \infty$ as $\omega \to 0$ for each model and for each k_2. This is also indicated by the analytical result given by equation (5.2.38). A Fig. 5.2.6(b) shows that for New model-2 and GN-III model, $\delta_T \to 0$ as $\omega \to \infty$. However, New model-I, predicts that $\delta_T \to$ constant value as $\omega \to \infty$, although this limiting value is very close to zero. This is in agreement with analytical result (see equation (5.2.36): for New model-1 $\delta_T \to \frac{1}{\sqrt{C_1}}$ which is equal to 0.005 for $k_2 = 1$).

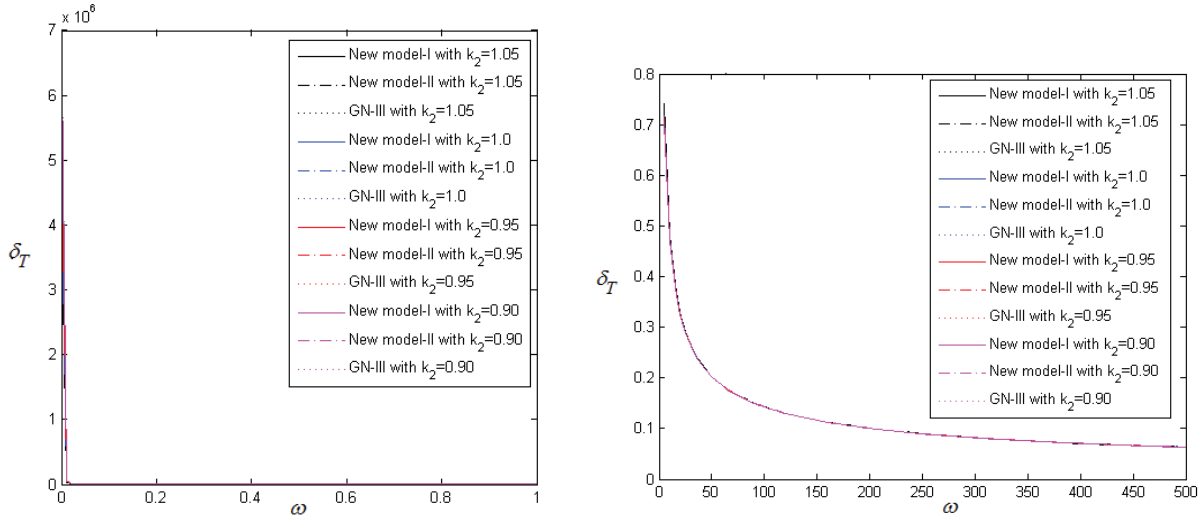

(a) (b)

Figs. 5.2.6(a,b): Variation of penetration depth of elastic wave δ_T with low and high frequency (ω) respectively

Amplitude ratio:

The behavior of amplitude ratio for mode elastic mode longitudinal wave is observed from the Figures 5.2.7(a,b). From Fig. 5.2.7(a) we see that there is not much difference in ψ_E for low frequency value of ω. For all the models, $\psi_E \to 0 \; as \;\; \omega \to 0$. But for the case when $k_2 \leq k_1$, all the models show some local maximum value before reaching to its limiting value. The value of the critical frequency varies with k_2. In Fig. 5.2.7(b), we observe that for very high frequency values i.e when $\omega \to \infty$ we have $\psi_E \to 0$ (also verified from analytical result) for New model I, but it decreases towards zero very slowly. In the cases of New model II and GN-III, it tends to a constant value. It is also verified by analytical result (see equation (5.2.44)) that for New model II, its value is $\frac{B_1'}{a_1}$, which is approximately equal to 0.2548 for k_2=1. We further note that for different values of k_2 this limiting value is different.

In Fig. 5.2.8(a), we see that the nature of the amplitude ratio of thermal wave in low frequency case is almost the similar for all the three models. $\psi_T \to \infty \; as \;\; \omega \to \infty$ for all the three models. In the case when $k_2 \leq k_1$we see that under each model, it attains a local minimum value before reaching to its limiting value. The position of this critical point

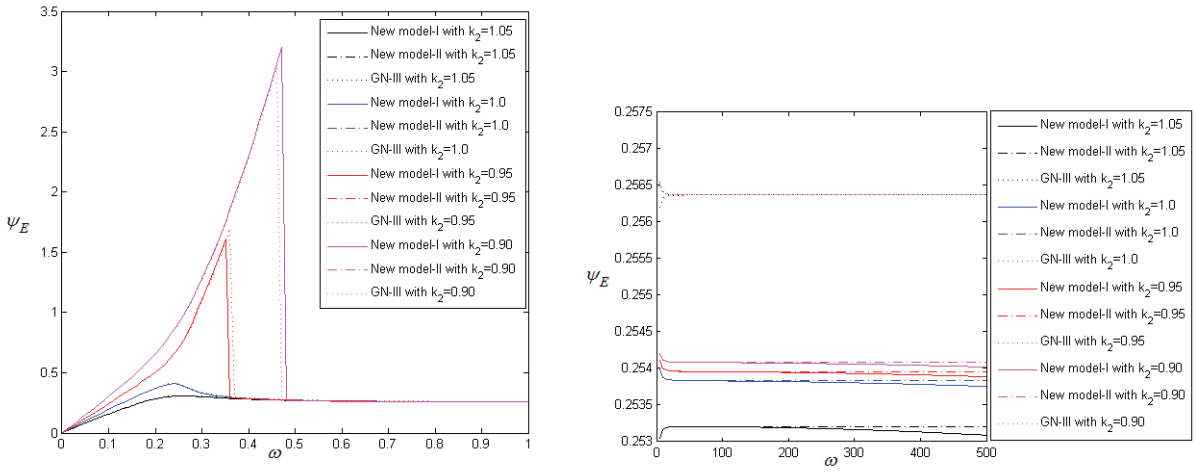

(a) (b)

Figs. 5.2.7(a,b): Variation of amplitude ratio of elastic wave ψ_E with low and high frequency (ω) respectively

varies with k_2. Figure 5.2.8(b) reveals that there is not much difference in the nature of the amplitude ratio of thermal mode wave under three models in high frequency case. All the models predict that $\psi_T \to \infty \; as \;\; \omega \to \infty$, which is also verified by our analytical result (see equations (5.2.43) and (5.2.45)). We do not observe any effect of k_2 in this case.

5.2.9 Conclusion

In this paper, we investigate the behavior of harmonic plane wave under the very recent heat conduction model with a single delay term introduced by Quintanilla (2011). We consider two types of Taylor series expansion of this new heat conduction model and refer them as New model-I and New model-II. Asymptotic results of the dispersion relation solutions for both high and low frequency values are presented here for both the models. Also, the asymptotic expressions for the important wave components like, phase velocity, specific loss, penetration depth and amplitude ratio are derived for both New model-I and New model-II with the variation of frequency and the thermal conductivity rate. We present both analytical and numerical results for a thorough comparison. We show that the analytical results are in perfect match with numerical results. We further compare our

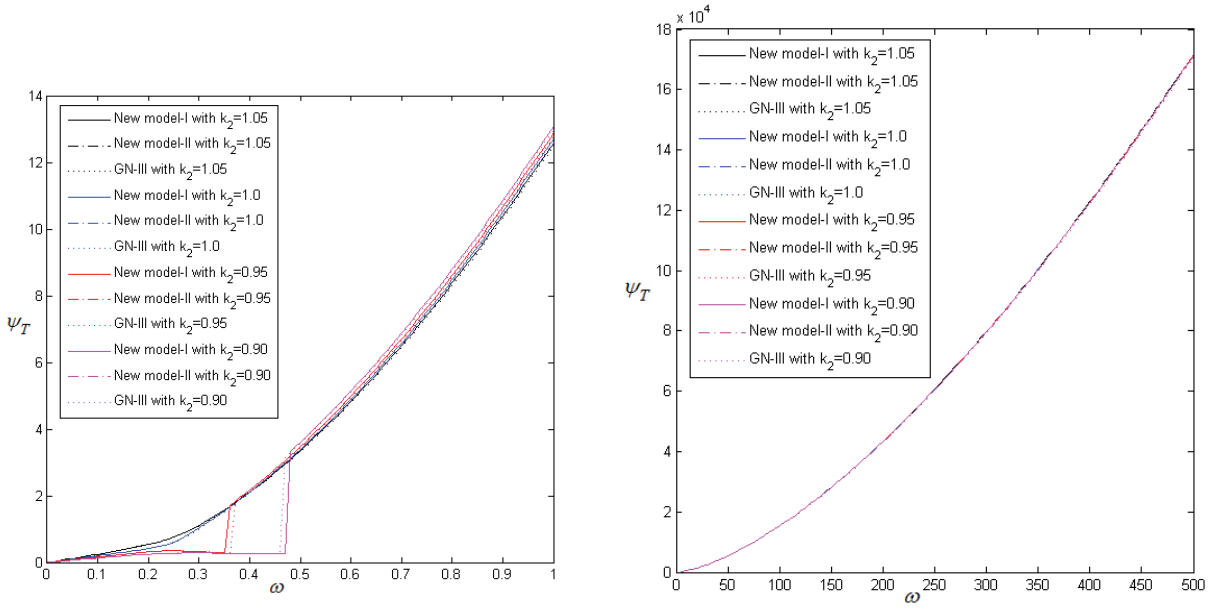

(a) (b)

Figs. 5.2.8(a,b): Variation of amplitude ratio of elastic wave ψ_T with low and high frequency (ω) respectively

results with the corresponding results of Green-Naghdi thermoelasticity theory of type-III. We observed following significant facts:

(1) We see that under all the models, only the longitudinal wave is coupled with the thermal field and there are two different modes of the longitudinal wave. One is elastic and the other one is thermal in nature.

(2) For lower frequency values, we observe from analytical and numerical results that all the model show the same nature for all important wave components. But for different values of thermal conductivity rate, there is a significant difference in the results under each model. In case of elastic wave, each model attains its local maxima and in case of thermal wave it attains a local minimum before tending to its constant limiting value.

(3) For higher frequency values, there is variation in nature of New model I and New model-II. In this case, New model-II is much closer to GN-III model. There is not much significant change in the nature of each model after taking different value of k_2.

(4) We also observe that the effects of the material constant k^* are more prominent for

lower values of frequency and the effects of the term τ^2 are more significant for higher values of frequency.

(5) As $\omega \to \infty$, we find that $V_E \to$ *constant* under each model, whereas $V_T \to \infty$ as $\omega \to \infty$ in all cases.

(6) The theoretical as well as the numerical results indicate that in case of New model-I, the specific loss of thermal mode wave is an increasing function of ω and approaches to infinity as $\omega \to \infty$. However, this field approaches to a constant limiting value under New model-II and GN-III models.

(7) We have $\delta_E \to \infty$ and $\delta_T \to$ *constant* as $\omega \to \infty$ for New model -I, whereas $\delta_E \to$ *constant* and $\delta_T \to 0$ in the contexts of other two models.

(8) As $\omega \to \infty$, $\psi_E \to 0$ under New model -I and $\psi_E \to$ *constant* under other two models, whereas $\psi_T \to \infty$ under all the three models.

(9) New model-II and GN-III model predict more similar results.